RC22737 (W0303-012) March 5, 2003
Materials Science

IBM Research Report

Atomic Layer Deposition of Metal and Nitride Thin films: Current Research Efforts and Applications for Semiconductor Device Processing

Hyungjun Kim
IBM Research Division
Thomas J. Watson Research Center
P.O. Box 218
Yorktown Heights, NY 10598



Research Division
Almaden - Austin - Beijing - Delhi - Haifa - India - T. J. Watson - Tokyo - Zurich

LIMITED DISTRIBUTION NOTICE: This report has been submitted for publication outside of IBM and will probably be copyrighted if accepted for publication. It has been issued as a Research Report for early dissemination of its contents. In view of the transfer of copyright to the outside publisher, its distribution outside of IBM prior to publication should be limited to peer communications and specific requests. After outside publication, requests should be filled only by reprints or legally obtained copies of the article (e.g. , payment of royalties). Copies may be requested from IBM T. J. Watson Research Center ,
P. O. Box 218, Yorktown Heights, NY 10598 USA (email: reports@us.ibm.com). Some reports are available on the internet at http://domino.watson.ibm.com/library/CyberDig.nsf/home .

 INNOSCIENCE EXHIBIT 1028

Atomic layer deposition of metal and nitride thin films: Current research efforts and applications for semiconductor device processing

H. Kim
IBM T.J. Watson Research Center, Yorktown Heights, NY 10598

Abstract

Atomic layer deposition (ALD) has been studied for several decades now, but the interest in ALD of thin metal/nitrides films has increased only recently. This is driven by the need for highly conformal nano-scale thin films in modern semiconductor device manufacturing technology. ALD is a very promising deposition technique with the ability to produce thin films with excellent conformality and compositional control with atomic scale dimensions. However, the application of ALD to metals and nitrides in real semiconductor device processes requires a deeper understanding about the underlying deposition process as well as the physical and electrical properties of the deposited films. This paper reviews the current research efforts in ALD for metal and nitride films as well as their applications in modern semiconductor device fabrication.

I. Introduction

Atomic layer deposition (ALD) is a self-limiting film growth method characterized by the alternate exposure of chemical species in layer-by-layer manner. ALD was developed in the 1970's by Dr. Suntola, and its first successful application was for the deposition of materials used for display devices.[1] Originally, the deposition technique was called atomic layer epitaxy, emphasized on the deposition of epitaxial films in high quality vacuum environments. Until early 1990's, ALD had been considered only for very limited applications such as the deposition of II-VI materials for display devices and III-V compound, or elemental semiconductor (Si, Ge) thin films.[1-5] The biggest limitation of ALD has been its low growth rate, leading to a potential problem in mass production. Thus, in most semiconductor or micro-dimension technical applications, ALD could not compete with other widely used thin film deposition techniques such as chemical vapor deposition (CVD) or physical vapor deposition (PVD).

However, with the continued scaling down in semiconductor devices, now clearly entering the nano-scale technical node, the need for a deposition technique to produce very conformal, ultra thin films at low growth temperatures has been increased.[6] In addition, the increase in Si wafer size to 300 mm requires deposition techniques with good, intrinsic uniformity. The process temperature limitation for all deposition technologies has become more severe by the introduction of novel low k materials for interconnect or "Back End Of the Line" (BEOL) applications. This restriction in deposition temperature depends strongly on the choice of low-k dielectric as well as the various integration schemes used in production. Generally, This puts an absolute upper limit on the processes of 400 ºC.

The need for ultra thin metal/nitride thin films in modern semiconductor technology comes from largely by the introduction of Cu interconnect technology. Although Cu has low

electrical resistivity and good electromigration resistance, the use of Cu as interconnect materials requires thin conducting layers in the structure which enhance the adhesion of Cu to dielectrics, prevent in-diffusion of O-containing species as well as diffusion of Cu into Si or dielectrics, and provide capability of electrodeposition of Cu. In addition, the Cu metallization has introduced new concepts in integration schemes for semiconductor device process, such as electroplating of Cu, chemical mechanical planarization (CMP), and dual damascene structures, all of which inevitably increase the complexity and scope of the metals and nitrides used in high aspect ratio structures at nanoscale dimensions.

The most widely used deposition technique for the diffusion barriers and adhesion/seed layers used in interconnect (BEOL) applications in modern semiconductor devices (> 100 nm nodes) has been sputter deposition from a magnetron cathode, which is known generically as PVD. There exist various derivatives of PVD, which have been developed to enhance the directionality or conformality of the deposited films, such as collimated or ionized PVD (I-PVD).[7,8] Even with these considerable improvements, PVD-based technology has an inherent limitation in the deposition of sub-100 nm, high aspect ratio structures due to the directional nature of depositing flux and high sticking probability on most materials.[9] The ITRS roadmap clearly indicates that new deposition techniques need to be introduced in the coming 5 years as the device technology node shifts to sub-100 nm range (Fig. 1).[6]

In summary, any new deposition techniques should provide 1) excellent conformality in nano-scale structures (<100 nm) with very high aspect ratio, 2) very good uniformity (<2%) for 300 mm Si wafers, and 3) good materials properties with minimum damage to the materials and 4) the growth temperature should be low enough for BEOL process. Considering these constraints and the clear need in semiconductor processing for atomic scale films, ALD is a very

promising techniques for a wide range of process considerations and device applications in near-future semiconductor technology. Thus, there is a real need for the development and understanding of ALD techniques for the appropriate metals and metal nitrides used along with the Cu as diffusion barriers and adhesion/seed layers. In addition, the dimensional scaling of metal oxide semiconductor field effect transistor (MOSFET) devices has led to the need for new gate/electrode materials and in high density DRAM structures, there is a requirement for a high aspect ratio metal electrode within the capacitor structure.

In addition to the early review papers on III-V, II-VI, or elemental semiconductors,[1-4] more recent review papers and manuscripts are available for general aspects of ALD.[5,10-13] However, the ALD of metal and nitride thin films and their application aspect in semiconductor device fabrication has been rarely reviewed. Thus, in this paper, the ALD process as well as the material characterization of metals and nitirides will be reviewed, with the primary focus on the applications in semiconductor devices including interconnects (BEOL) and front-end applications. The overall research status of these materials will be described along with future investigation directions. Among nitrides, dielectric nitrides such as silicon nitrides will not be covered, and although silicides are another important conducting film widely used in semiconductor devices, they will not be described here due to the lack of report on them.

II. Fundamentals of metal and nitride ALD

1. The ALD process

Atomic layer deposition of metals and/or nitrides consists of essentially four steps; 1) metal precursor exposure, 2) evacuation or purging of the precursors and any byproducts from the chamber, 3) exposure of the other reactant species (non-metal precursor), for example

nitrogen containing reducing agents for nitrides or reducing agents for metals, and 4) evacuation or purging of the reactants and byproduct molecules from the chamber. While the primary reaction between metal precursor and non-metal precursor occurs during step 3), reaction byproducts are formed also at the metal precursor exposure step (step 1). As an example of ALD process, a schematic representation of TiN ALD, which has been one of the most widely studied nitride ALD processes, is shown in Fig. 2. In this example, TiN ALD process using $TiCl_4$ as metal precursor and NH_3 as the reducing agent/nitrogen source is shown.[14-19] While this specific reaction sequence will be used in the following description, most other metal or nitride ALD sequences consist of generally similar process steps.

As a first step of TiN ALD, the nominally clean initial surface is exposed to $TiCl_4$ for a given time (Fig. 2a). The most widely used unit for the exposure is a Langmuir, which is defined as the exposure of any gas of one second at 10^{-6} Torr (1 Langmuir = 10^{-6} Torr s). Typical metal precursor exposures in ALD process use a level of several 10k Langmuirs, or the equivalent of several tens of mTorr pressure for one second. Creating an adequate flux of the metal precursor into the chamber depends strongly on the metal precursor used. For the case of a liquid source such as $TiCl_4$, the vapor pressure is high enough even at room temperature such that the precursor can be directly admitted to the chamber through a leak valve. In the cases of the most solid precursors, however, it is necessary to heat the chemicals to produce an adequate vapor pressure. Here, since excessively high temperature could result in decomposition of sources, care should be taken. In addition, the gas line between solid source volume and the chamber are usually heated at slightly higher temperature than precursor container itself to prevent the condensation of source vapor in the line. For most metal precursor delivery systems, a carrier gas such as Ar or N_2 is used for better transport of the metal precursor vapor. The flows of the

precursors (and carrier gases) are typically controlled by mass flow controllers (MFC) or conventional leak valves. Due to the automated, sequential, and fairly short time period of the precursor and reactant flows, the use of automated shut-off valves and fixed leak valves is often preferable to conventional MFCs, which are often designed for stable, steady-state flow control rather than pulsed operation. Other configurations are also possible for delivery of metal precursors. For example, a liquid injector can be used for the liquid source, or in some cases the precursors are solved in the solvent and a vaporizer is used. In any case, it is necessary that the precursors are allowed to adsorb on the surface until the saturation coverage is reached.

One of the most important requirements for this first step is the self-limitation for the precursor molecule adsorption process. Usually, this condition is satisfied by the ligands bonded to the metal atoms in the precursors, such as halogen or organic ligands. This limits further adsorption of the metal precursor by passivating the adsorption sites after the saturation coverage, roughly one monolayer or less, is reached. As Fig. 2a shows, $TiCl_4$ molecules do not adsorb on the surface sites covered by Cl atoms. The detailed mechanisms or kinetics of adsorption process for most metal precursors have been rarely investigated. Some precursors go through dissociative adsorption, while others adsorb intact, which often depends on the state of the surface as well as the growth temperature. At very low temperature, however, multiple layer of precursors can be adsorbed to the surface by condensation of precursors on the surface.

For TiN ALD, $TiCl_4$ molecules adsorb on the surface as a form of $TiCl_x$ ($x < 4$).

$$TiCl_4(g) \rightarrow TiCl_x(a) + (4-x)Cl(a) \quad (1)$$

However, the detailed surface reaction pathway is still unknown. A previous report has shown that $TiCl_4$ molecules adsorb molecularly on tungsten surface at 100 K, and then dissociate to $TiCl_3$ and Cl above 220 K.[20] At higher surface temperature, a more complicated reaction occurs

involving disproportionation, which results in various $TiCl_x$ species present on the surface. A recent study on a Si surface using scanning tunneling microscopy (STM) has shown that various surface species including $TiCl_4$, $TiCl_2$, Ti, and Cl can exist simultaneously on a Si(001) surface at room temperature.[21] Thus, the whole adsorption process at room temperature and above can not be adequately explained by one simple kinetic equation.

Ideally, one monolayer of the metal precursor adsorbs on all exposed surfaces within the vacuum chamber during the exposure. However, in reality, the saturation coverage of a specific precursor is determined based upon various conditions including the size of molecules, deposition temperature, and the presence of byproducts from earlier reactions. Usually, the saturation coverage of the metal-containing precursor for most metal and nitride ALD reactions is far less than the desired monolayer (ML). One of the most widely accepted reason is steric hindrance of adsorbed metal precursors as proposed for TiN ALD.[16] But not every case can be explained simply by steric hindrance.

At the second step, the remaining precursor gas and any byproducts ($TiCl_4$ and HCl in this example) in the chamber are evacuated. (Fig. 2b) Usually, a purging gas such as argon or nitrogen is used to help complete removal of precursors and/or byproducts. For some cases, particularly in manufacturing applications where there is a concern both for high rate operation as well as particulate suppression, a continuous flow of purging gas even during step 1) and 3) can be used to assure fast removal of these gases. The purging step is also required to eliminate potential CVD-like processes, which can occur when the reactant gas is introduced in the presence of the precursor in the gas phase. This perturbs the ALD growth mode and leads to potential inclusion of byproduct species in the film, as well as the loss of conformality. While chemistry of CVD-like process is intrinsically similar to ALD, the fundamental advantages of the

ALD approach in terms of thickness and composition control and film uniformity are such that the CVD mode is generally avoided in most cases.

At the third step, non-metal precursor (NH_3 in this example) is introduced into the chamber. (Fig. 2c) For these non-metal reactant species, which are usually gas phases, MFC or a switched leak valve is used for the control of the flow. For TiN ALD, the Cl atoms on the surface, either as adatoms or as part of the $TiCl_x$ fragments, react with NH_3 and the byproduct HCl is produced,

$$TiCl_x(a) + NH_3(g) \rightarrow TiNH_{3-x}(a) + xHCl(g)\uparrow \quad (2)$$

In this process, N atoms bond to the Ti on the substrate, resulting in TiN deposition. For metal deposition, a reducing agent such as atomic H is used for removing Cl from the surface generating fresh surface for further adsorption at the next deposition cycle.[22]

At the fourth and last step, all the remaining NH_3 (or hydrogen) and HCl are swept away by evacuation or purging. (Fig. 2d) Additionally, it is necessary to differentiate between the first step of the ALD process on a clean substrate surface, and the same exposure step at a later cycle when the surface consists of the previously deposited film from prior reactions. For the latter case, $TiCl_4$ reacts with NH_y surface species adsorbed from the fourth step of last cycle. Thus, HCl is formed as byproduct from the reaction between NH_y and incoming $TiCl_4$ molecules.[23]

$$NH_y(a) + TiCl_4(g) \rightarrow NTiCl_{4-y}(a) + yHCl(g)\uparrow \quad (3)$$

The understanding of detailed mechanisms during each of the four steps requires an extensive amount of surface science, measurement of the reaction kinetics, and study of the mass transport. Overall, extra care should be taken to ensure that the whole process occurs in the ALD mode growth. The most common mistakes causing non-ALD growth include: a) insufficient precursor exposure, which results in non-saturated adsorption, b) insufficient purging or

pumping time in steps 2) and 4), which allows either residual metal precursor molecules in the system during the reactant gas exposure or reactions during the metal precursor exposure which limit precursor adsorption, both of which can result in CVD-like growth, or c) deposition at too lower or higher growth temperature, resulting in smaller or faster deposition rates than expected.

2. Characteristics of ALD

There are many similarities between ALD and CVD. For example, both techniques use a gas phase precursors and chemical reactions between them are the primary thin film deposition mechanism. In addition, the precursors used are often identical. Accordingly, the physical configuration of the ALD and CVD reaction chambers is usually very similar. In fact, ALD can be thought as a modified version of CVD and for this reason ALD has been also called Atomic Layer CVD (AL-CVD). However, the clear, distinctive features of ALD include the self-limited growth mode and the alternate, sequential exposure of the precursor and reactants, resulting in several unique characteristics for ALD, which are not found in CVD.

For example, the growth rate as a function of sample temperature or precursor flux shows clear differences between the two deposition techniques. For conventional CVD, the growth rate is a strong function of substrate growth temperature at low temperature, where the growth rate is determined by surface reactions (surface reaction limited regime). In this regime, the growth rate increases exponentially with increasing growth temperature, since the available adsorption site density is determined by an Arrhenius-type reaction. At high temperature, however, the growth rate becomes constant with respect to temperature if the mass transport or gas phase diffusion does not limit the process. (flux limited regime). As an example, typical ultra high vacuum CVD (UHV-CVD) type Si growth rates as a function of growth temperature are shown in Fig. 3.[24] As

Fig. 3 shows, the growth rate of CVD increases with increasing precursor flux until the process is governed by the delivery of the source gases. Thus, precise control of the flow of the metal precursor and reactant gases is critical to the reaction rate and effective deposition rate, and the thickness control for very thin films is limited especially in flux-limited regime. Moreover, in surface reaction limited regime, since the deposition rate is an exponential function of growth temperature, the reproducibility in film thickness relys on the precise control of growth temperature, which is often difficult in production type chamber configuration. In addition, due to the direct gas phase reaction between precursors, which can occur during the deposition process, there is high probability of particle formation.

The growth rate of typical ALD process follows the pattern shown in Fig. 4 as a function of growth temperature depending on the materials system, as also pointed out previously.[10] In many cases, the growth rate increases with increasing growth temperature at low growth temperature (typically below 150-300 ºC for metals/nitrides ALD). This is mainly because the precursor adsorption or reaction between precursor and surface species is thermally activated process. Thus, the saturation reaction is kinetically limited with low thermal energy, which would lead to impractically long reaction time.[10] This kind of behavior has been reported for many metal/nitride ALD. For example, deposition rate rapidly drops below 150 ºC for W ALD using WF_6, which was attributed to the incomplete reaction at this low growth temperature.[25] Similarly, the growth rate of Ta_3N_5 thin film deposition by ALD using $TaCl_5$ precursor was observed to decrease below 300 ºC.[26] For some cases, the trend shows opposite behavior, when the metal precursors condense on the substrates, as mentioned in the previous section. However, this can be hardly considered as real thin film deposition. When the ALD process is operated at temperatures providing high enough thermal energy without condensation for the reactions, the

growth rate remains constant with respect to the growth temperature. This temperature range is often called as “ALD process window”. The existence of this process window provides easier control in terms of reproducibility for the growth rate during ALD compared to CVD. At higher growth temperature above process window, however, the growth rate usually increases again with growth temperature, due to the disturbance of self-limitation caused by thermal decomposition of the metal precursor, causing a CVD-like process. While this thermal decomposition is not usually a problem for halide precursors due to their relatively high thermal stability, metal organic (MO) sources can be decomposed at relatively low growth temperature. For some cases, the growth rates decreases with increasing growth temperature when the thermal desorption of deposited materials occur. However, this has been seldom observed for metals/nitrides ALD. In real cases, additional reaction such as etching of deposited materials by precursors or disproportionation often makes the behavior more complicated.

Within the temperature process window and under the saturation condition, the growth rate of ALD does not increase with increasing precursor flux. Fig. 5 shows a typical example of this behavior for Ta plasma-enhanced ALD using $TaCl_5$ and atomic H. In this case, the effective number of Ta atoms deposited per cycle increases with increasing $TaCl_5$ exposure time for times less than 1 sec, but when it reaches apparent surface saturation, the growth rate per cycle remains unchanged even with a large increase in precursor exposure.[27] Thus, the overall growth rate during ALD is predetermined and stabilized by the surface saturation limitation, and the exact control of the precursor flux is not critical compared to CVD. This, together with process temperature window, is a great process advantage for manufacturing applications, where it is not usually possible to measure the thickness of the deposited film on each sample. Thus, ALD film has potentially better reproducibility in thickness compared to CVD.

An additional, practically more important benefit of intrinsic self-limitation of ALD due to surface saturation is excellent step coverage on aggressive topographic structures on the surface. This is one of the most important driving forces for the recent intensive interest in ALD for microelectronics. In an ALD process, the surface saturation effect occurs on all surfaces, which receive an adequate flux of the metal precursor. Thus, with long enough exposure time, nearly 100% conformality in very high aspect ratio (AR = feature depth/width) structures is easily achievable. In contrast, the conformality of PVD technique is intrinsically limited by the directional nature of the sputtered atoms and the near-unity (in many cases) sticking coefficient for the metal atoms.[8] If PVD depositions are made to be very directional as in case of collimated PVD, poor sidewall coverage is resulted on deep features. If the directionality is reduced, sidewall coverage can be increased but there is a tendency to produce overhangs in the deposited films near the top corners of features, which can limit subsequent process steps. Because of the directional nature of PVD, conformality is limited to usually less than 20%. A typical thin film thickness profiles on high aspect ratio structure deposited by collimated and ionized PVD are depicted in Fig. 6.

Although CVD can produce better conformality than PVD in some systems, there is an intrinsic flaw relating conformality to film composition or continuity in very thin films. Due to the flux-controlled nature of CVD, conformality in deep features can only be achieved with a low reaction probability (at low growth temperature of surface reaction limited regime). This same feature inhibits film nucleation and can result in poor continuity at the sub-5nm thickness regime desired for many applications. In addition, the low reaction rate can lead to impurity incorporation either from non-reacted precursors or poor removal of byproducts.

Since ALD is inherently layer-by-layer, self-limited deposition process by the alternate exposure of two or more precursors, thickness and composition control is feasible at the sub-monolayer or even atomic level. Thus, ALD is an ideal deposition technique to construct nanolaminate structures. In fact, ALD has been employed for superlattice structure formation of compound semiconductors from the early history of ALD.[12] Recently, high k oxide nanolaminates deposited by ALD with exact thickness and composition control have been intensively studied due to the expected good property for CMOS FET application with very thin gate oxide.[28,29] Until now, the nanolaminate structure of metals and nitrides by ALD has been rarely studied, probably due to the lack of urgent need in device applications. Only recently, TiN-Al and Al_2O_3-W nanolaminate have been grown by ALD.[30,31] Transition electron microscopy (TEM) image of the Al_2O_3-W nanolaminate prepared by ALD is shown in Fig. 7.[31]

Other advantage of ALD compared to CVD is a possibility of the simpler reactor geometry. Many typical CVD processes occur at flows of many hundreds of sccm and at static operating pressures in the mTorr to Torr regime. At these pressure ranges, gas conduction is limited by the geometry of the vacuum system. Due to this problem, great care must be taken to introduce the gases uniformly as well as pump the chamber symmetrically. The gases are introduced through showerheads, which adds complexity to the system and are prone to clogging and particle formation. ALD processes, however, typically operate in the near-molecular flow regime (and for short periods only) and as such, there is less need for showerheads and issues concerning gas distribution are relatively small. The nonuniformity of the ALD process in the molecular flow regime should be better than a few percent, and batch processing of wafers is feasible.[32]

Another characteristic of ALD is the generally lower growth temperature compared to the parallel CVD reaction. Since the adsorbed monolayer is reacted to completion, there is often a much lower impurity level in the deposited film compared with CVD. This is related to the fact that the ALD process occurs exclusively through surface reactions. For CVD, except for several special cases (such as UHV-CVD, for example), vapor phase chemical reaction is the main reaction mechanism, which is a common source of particle formation in CVD reactors. In addition, since ALD occurs through surface reaction, the selectivity of deposited materials could be controlled by proper selection of precursors. Although the successful selective ALD for metals/nitrides has not been demonstrated yet, it is anticipated that this will be demonstrated in the near future.

The growth rate of ALD is very low compared to virtually all other deposition techniques. At best, the thickness/cycle in the typical ALD mode is limited to below 1 ML/cycle. For practical vacuum systems, the total time for 1 cycle (4 steps) is at least 1 sec. This corresponds to the deposition rate of 1 μm/hr or below (a few tens of Angstroms per minute). Moreover, the actual deposition thickness/cycle is a small fraction of ML per cycle for most metal and nitride ALD. In recent applications in microelectronics, however, the required thickness of metals and nitrides films has become very small, in the low nm range, and this resulted in the low growth rates of ALD more acceptable. For example, for the 65 nm interconnect generation, the Cu diffusion barrier thickness can be no more than 5 nm thick, which can be deposited with less than 100 ALD cycles. Thus, the required film can be grown within a several minutes, leading to a wafer chamber throughput of perhaps 20 wafers per hour (w.p.h.). Moreover, batch process can further reduce the required average process time/wafer as pointed out above.

As another approach to increase the wafer throughput, modifications of the ALD process have been attempted. This kind of controlled CVD-like process can be achieved by reduction of the purging time, deposition at a higher growth temperature, or mixing of the precursor and reactant species at the same cycle. The film quality in this latter mode and the conformality are expected to be worse than ALD steps, but this hybrid process shows improvement in the net deposition rate compared to ALD and improvement in the film conformality compared to CVD. This kind of modified ALD techniques are called with different names such as pulsed nucleation layer deposition, nano-layer deposition, or cyclic CVD.[33-35] In addition, the thermal or plasma enhanced cracking of the metal precursors, if well controlled, could result in enhancement of growth rate.[36]

3. PE-ALD

As mentioned briefly in the previous section, activation energy is usually required for precursor adsorption on the surface and/or the exchange reaction between the precursor and surface species. For conventional ALD, this energy is provided thermally by heating the substrate. Thus, the conventional mode of ALD is also called thermal ALD, where the substrate or entire chamber is heated. For thermal ALD of metals or nitrides, the typical temperature process window usually corresponds to 300 – 500 °C for halide sources and 150 – 250 ºC for MO sources. For thermal ALD, the precursors are introduced into the chamber at constant sample temperature. One exception is known as “temperature modulation” technique, in which the metal precursor is adsorbed at lower temperature and substrate temperature is quickly raised to produce further adsorption sites. However, due to the technical difficulty of implementing

rapid changes of the sample temperature, this method has only been tried for limited cases, such as ALD of elemental semiconductor.[37]

Alternative methods to provide the required energy have been attempted to enhance ALD. For example, photon induced heating (photothermal) or direct excitation by photon (photolytic) have been used for deposition of elemental semiconductor in laser assisted ALD of Si.[38] However, there are no comparable reports for ALD of metals or nitrides. Instead, plasma enhanced ALD (PE-ALD) has been the most widely used technique as alternative method to thermal ALD for the metals and nitride thin film deposition. PE-ALD is also called radical enhanced ALD (RA-ALD) or plasma assisted ALD (PA-ALD).[39,40] Generally, PE-ALD produces better quality film at lower temperatures, since the required activation energy is provided by plasma source. Although the substrate should be heated, the required growth temperature is significantly lower than thermal ALD.

Compared to the conventional thermal ALD, the chamber configuration is rather complicated due to the requirement for a plasma source. Plasma can be generated by several ways, including rf, microwave, and electron cyclotron resonance (ECR). A schematic of an example system for rf-plasma based PE-ALD is shown in Fig. 8. As table 3.1 shows, only a limited number of metals or nitrides have been deposited by PE-ALD. Although PE-ALD is in very early stages of development, many references are available for plasma enhanced CVD (PE-CVD).[41,42] For PE-CVD, there have been two different configurations, remote or direct plasma, depending on the position of plasma source. For remote PE-CVD, gas species are excited remotely outside (upstream) of the chamber in a separate excitation chamber, and the generated radicals are introduced to the chamber downstream. For direct plasma CVD, plasma is generated inside of the chamber and all precursors and reactants are excited altogether.

In a parallel mode, both remote and direct type PE-ALD configurations have been tried. However, in contrast to the typical PE-CVD, only the non-metal precursors are activated for PE-ALD. The main reason is that excitation of metal precursors causes cracking of gas molecules, resulting in the disturbance of the self-saturation of adsorption which is a basic requirement for ALD. One of the most widely used PE-ALD methods has been the excitation of molecular hydrogen by plasma.[43] Plasma activation of gas species easily produces large quantities of highly reactive species such as atomic H. The generated atomic hydrogen, which is a strong reducer, reduces the metal precursors on the sample surface to produce metal films at relatively low growth temperature. While the diagnosis or monitoring of the plasma is often possible by optical emission spectroscopy (OES), detailed study has been rarely performed between the plasma characteristics and ALD film properties.

The first reported result of PE-ALD was using atomic H generated by rf plasma to grow transition metal thin films, including Ti and Ta, which cannot be deposited by thermal ALD at low growth temperature.[43] The Ta films with Cl content below 0.5 % was deposited by PE-ALD at sample temperatures below 250 °C.[27] By this process, Ta film deposition was possible even at room temperature. The Cl contents in PE-ALD Ta films are shown as a function of growth temperature and hydrogen exposure time in Fig. 9. More recently, by using the mixture of hydrogen and nitrogen plasma, cubic TaN thin films have been deposited at low growth temperature. [44] This capability for low temperature growth is beneficial for semiconductor device applications, especially for interconnect applications, which requires process temperature below 400 °C. Another benefit of PE-ALD is the improvement of the deposited material properties. For example, when $(N(Et)_2)_3Ta=N^tBu$ (tert-butylimidotris(diethylamido)tantalum, TBTDET; Et = C_2H_5, ^tBu= $C(CH_3)_3$) and NH_3 are used for TaN thermal ALD, the resultant films

had high resistivity (>20k μΩcm) and very low density (3.6 g/cm^3).[45,46] In the PE-ALD case using TBTDET and atomic H produced by plasma, however, the resistivity of TaN thin films was as low as 400 μΩcm and the density increased to 7.9 g/cm^3.[46] Additionally, during PE-ALD, bias can be applied to the substrate, potentially producing other effects on or changes in the stoichiometry or density of the deposited films. However, little study has yet been reported for the effect of bias during metals or nitrides PE-ALD.

In the process point of view, PE-ALD could have more limitations or complications than thermal ALD, which are mainly due to the high reactivity of the radicals produced by plasma. For example, a Si substrate can be etched by atomic H at certain temperature range.[47] This resulted in etching of Si substrate rather than deposition of a film on it at the early stages of Ti PE-ALD.[22] In addition, some low k, polymer-based materials may be damaged by the atomic H species, which could limit the use of hydrogen plasmas. As an another process related issue, there is a concern about recombination of the active species produced by plasma, such as atomic H or nitrogen.[48] This could result in spatial nonuniformity across the chamber or perhaps in deep vias or trenches due to a reduction in the effective flux of the reactive species (H) after multiple surface or wall collisions. Thus, the conformality of PE-ALD film could be limited in very high AR structure, although 100 % conformality has been reported for PE-ALD Ta in trench structure with AR up to 15.[27]

4. Precursors

The precursors used for ALD should have high enough volatility and stability against self-decomposition, go through aggressive and complete reactions, cause no etching reactions, not be dissolved to the film or substrates, and produce stable, non-reactive volatile by-

products.[10] Table 3.2 summarizes the reported precursor combinations, which have been used for ALD of metals and nitrides. Usually, for elementary metal ALD, the metal-containing precursors are reduced by other non-metallic precursor (reducing agent) to produce the metal film. However, special cases have been reported recently. For example, Ru and Pt ALD was performed by direct reaction between metal precursor and molecular oxygen, where the ALD occurs by oxidative decomposition of metal precursors.[49,50] And Ni and Pt were obtained by reducing the metal oxide deposited by ALD using a metal precursor and an oxidant.[51] For nitride ALD processes, the general approach is to use a MO source which is reduced with ammonia or atomic hydrogen, [45] or to use a halogen source which can then be reacted with ammonia or combinations of hydrogen and nitrogen.[44] Among these, the most general method is using NH_3 or other non-metal precursor as nitrogen source as well as reducing agent. The typical example is TiN ALD using $TiCl_4$ + NH_3, as described in the previous section. For both metal and nitride ALD, additional reducing agents such as Zn or $Al(CH_3)_3$ (trimethyl aluminum, TMA) have been tried to provide more reducing power.[16,52]

4.1. Metal precursors

Compared to ALD of metal oxides, a relatively small number of precursors have been used for metals and nitride ALD. (Table 3.3) This is mainly because the research on metal/nitride ALD is at its early stage and some oxygen containing metal precursors such as alkoxides could result in the oxygen incorporation during film deposition. The most widely studied metal precursors for metal/nitride ALD are halides, such as chlorides, bromides, iodides, and fluorides. Although halides are readily available and the deposition chemistry is relatively simple, most of the halides are solid at room temperature and have low vapor pressure. The exceptions are WF_6

and $TiCl_4$, which are liquid at room temperature with high vapor pressure. Thus, these two precursors have been popular for CVD/ALD processes. For ALD, however, due to its intrinsic self-limitation characteristic, low vapor pressure of solid precursors is not as great a concern compared to CVD. Rather, the negative effect of halogen contamination to the films is of greater concern. For example, the Cl residue in ALD diffusion barrier films could lead to corrosion problems in Cu metallization. Also, for halogen-based ALD without using plasma enhancement, usually a growth temperature well over 400 °C is required to produce metals/nitirides with low levels of halogen impurities. While halide precursors react with NH_3 to produce nitrides such as TiN, W_2N,[16,19] ALD of transition metal silicon nitrides have been achieved by addition of a Si source (for example, SiH_4).[53] However, for transition metal ALD including Ta or Ti, successful thin film deposition by halide sources has been achieved only using plasma enhancement.[43] For now, tungsten has been the most successful elemental metal deposited by thermal ALD using WF_6 as metal precursor.[25]

Metal organic (or organometallic) compounds are the other group of metal precursors, which have been extensively studied for CVD. The advantages of MO precursors are the high volatility and the low growth temperature. Alkylamides are the most widely used MO sources for transition metal nitride ALD. For example, $Ti[N(Me)_2]_4$ (tetrakis(dimethylamino)titanium, TDMAT; Me = CH_3) or $Ti[N(EtMe)_2]_4$ (tetrakis(ethylmethylamino)titanium, TEMAT) and NH_3 are representative set of precursors for TiN MO-ALD.[54-58] The growth rates are usually higher than halides based ALD and sometimes close to the ideal value of 1 ML/cycle (or higher). However, the incorporation of C and low density of the grown films are potentially significant problems. The low density of the film may be partially improved by plasma densification.[45] For metal ALD, diketonato complexes such as $Cu(thd)_2$ [Bis(2,2,6,6,-tetramethyl-3,5-

heptanedionate)copper(II); thd = $C_{11}H_{19}O_2$] or $Cu(hfac)_2 \cdot xH_2O$ [copper(II)(hexafluoro-acetylacetonate)·hydrate; hfac = $CF_3COCHCOCF_3$] were used for Cu ALD.[59,60] Recently, cyclopentadienyl (Cp = C_5H_5) compounds and O_2 were used for ALD of noble metals.[49] Other group of precursors such as alkyl compounds, alkyloxides, or carbonyls have not been tried for metal or nitride ALD. However, ALD using MO sources are still in the very early stages of development and it is expected that more precursors will be available for metals and nitrides ALD in the near future.

4.2. Non-metal precursors: Metal ALD

Typically, a metal ALD process is composed of adsorption of metal precursors on the substrates and the reduction of adsorbed precursors to metal films by proper reducing agents exposure. The most readily available and simplest reducing agent is molecular hydrogen. The typical reaction can be written as

$$ML(a) + 1/2H_2 \rightarrow M + HL(\uparrow), \quad (4)$$

where L can be either halogen or organic ligands depending on the metal precursors used. The first metal ALD to use this approach was Cu ALD using CuCl and H_2.[61] However, the use of H_2 as reducing agents usually requires high growth temperature. For example, CVD of Ta using $TaCl_5$ and H_2 is known to require a high growth temperature over 700 °C.[62] This high temperature is mainly due to the strong covalent bond between H atoms in H_2 molecule. In PE-ALD, cracking of molecular hydrogen is achieved using a plasma discharge, where the atomic hydrogen is produced by energy supplied from plasma. So far, Ta, Ti, and Sn films have been deposited by reaction between halides and atomic hydrogen.[22,27,43,63] In fact, the reducing capability of atomic hydrogen is such that if the proper amount of halides vapors could be

generated and fed into the chamber, most of the metals are expected to be deposited by atomic hydrogen reduction at moderate sample temperatures.

Metallic Zn vapor, which is generated by high temperature heating of Zn containing boat inside the chamber, is another powerful reducing agents for producing metal films for ALD. Mo films were deposited using $MoCl_5$ and Zn.[64] However, metallic Zn was found to reside in the film and cause CVD-like reactions. The same observation was reported for Cu ALD using CuCl and Zn.[61] In addition, Zn contamination could be problematic to the device performance, so the use of Zn vapor for semiconductor device process has practical limitation.

Si_2H_6,[25] SiH_4,[33] and B_2H_6[65] has been employed for tungsten ALD with WF_6. In this case, the reactant molecules reduce adsorbed tungsten fluoride to tungsten metal film while the Si atoms are not incorporated during deposition. Here, Si and F atoms are removed by desorption as SiH_xF_y molecules. No deposition of other metal film has been reported by this way. For $TaCl_5$, alternate exposure of $TaCl_5$ and SiH_4 produced $TaSi_2$, rather than metallic Ta.[53] For some special cases, molecular oxygen or air was used as a non-metal precursor to produce metal films (Ru or Pt)[49,50] or O_3 or H_2O to produce metal oxide films then the produced oxide has been reduced to metal films (Ni)[51,66].

4.3. Non-metal precursors: Nitride ALD

For nitride ALD, two sources are required in addition to metal precursor; a nitrogen source and a reducing agent. NH_3 has been the most widely used non-metal precursor, which plays a role as both nitrogen source and reducing agent, and has been used to produce wide range of nitride films by ALD, including TiN, Ta_3N_5, W_2N, NbN, and MoN_x.[14,67,26] Among these, the most intensively studied is the producing of TiN by the reaction of $TiCl_4$ and NH_3. This reaction

occurs above 320 ºC, but temperature higher than 400 ºC is required to obtain low Cl content below 1 %.[17] However, for tantalum nitride deposition, the reducing power of NH_3 is not high enough to produce desirable cubic TaN. Instead, high resistivity Ta_3N_5 phase is formed.[26] For low resistivity cubic TaN deposition, an additional reducing source has been employed including Zn and TMA.[26,68] Meanwhile, NH_3 with MO tantalum source such as TBTDET produced high resistivity amorphous phase.[45]

Other nitrogen containing reducing agents have been tried for nitride ALD. One of NH_3 alternative, $(Me)_2NNH_2$ (1,1-dimethylhydrazine, DMHy), was reacted with several different chlorides to deposit nitrides by ALD.[67] However, significant improvements in the ALD process or film properties were not obtained compared to NH_3. Similarly, amines including $^tBuNH_2$ (tertbutylamine) and $allylNH_2$ (allylamines; allyl = CH_2CHCH_2) have also been tried for the same purpose.[69]

For metal organic sources containing nitrogen in them, such as TBTDET for TaN and TDMAT for TiN, plasma-produced atomic H was used to deposit nitrides by PE-ALD.[45,70] In this case, the nitrogen in the precursors plays a role as a nitrogen source in the resulting nitrides film. In contrast, for PE-ALD using metal precursor without nitrogen in them, an additional nitrogen source must be provided, as in case for TaN deposition of PE-ALD using $TaCl_5$ as metal precursor.[44] For this study, activated nitrogen generated by the plasma was used as nitrogen source while atomic H is used for removing Cl atoms from the surface.

For ternary nitrides such as $TaSi_xN_y$, $TiSi_xN_y$, or $TiAl_xN_y$, a third precursor such as SiH_4 for Si[53,55] and Me_2AlH-EPP (dimethylaluminumhydride-ethylpiperdine, DMAH-EPP; EPP = $C_7H_{15}N$)[72,73,74] for Al is added. Usually, the change in sequence exposure of three precursors results in change in the deposited film properties.[53]

III. Potential applications of ALD metal and nitride thin films

The largest driving force for the recent development of metals and nitrides ALD is the need for ultra thin films with excellent conformality in nanoscale semiconductor device processing, especially for interconnect applications. In integrated circuits, the signals to the devices propagate through metal lines and vias embedded in an interlayer dielectric (ILD). The embedded lines have an electrical resistance related to their length and cross-section dimension, and the resistivity of the material used; typically Cu. In addition, the lines are capacitatively coupled via the dielectrics, resulting in an effective capacitance. The electrical signal through this circuit is constrained by the resulting RC delay, which is represented by RC time constant, which is approximately related to[(75)]

$$RC = (\rho/t_M)(L^2\varepsilon_{ILD}/t_{ILD)} \quad (5)$$

where ρ and ε is the resistivity of interconnect metal and dielectric constant of ILD, which are material dependent properties, while t_M, t_{ILD}, and L are thickness of metal and ILD layer and L is the length of the structure, all of which are determined by device geometry. As the device size shrinks, t_M and t_{ILD} decrease accordingly and the RC time constant increases according to the above equation. In order to compensate this effect, a decrease in ρ and ε is required. Thus, a number of the current research efforts in manufacturing for interconnect or BEOL features are mainly focused on low resistivity metallization materials (such as Cu) and low k dielectrics. In addition to this, there are other aspects of circuit performance and optimization, such as cross-talk and power dissipation, but those are not discussed here.

The most promising metallization scheme appears to be the use of Cu as the primary conductor in the majority of the interconnect features. Cu has low electrical resistivity (1.67

μΩcm), which is only slightly inferior to Ag (1.6 μΩcm) and lower than Au (2.3 μΩcm) or Al (2.69 μΩcm). Compared to the conventional Al interconnect, the resistivity decrease by using Cu is about 37 %, while the difference between Ag and Cu is only 5 %. Although Ag has the smallest resistivity among all metals, Ag is very fast diffuser into dielectrics as a form of ions. Cu is also a fast diffuser, but not worse as Ag or Au. Moreover, Cu has well established deposition technique such as electrodeposition, as described later. Another important aspect of metals for interconnect application is electromigration (EM) properties. Al has served as primary interconnect material for several decades in most of integrated circuits, but pure Al has significant electromigration problem, which is the most important reliability issue in device performance. EM is a mass transport phenomenon of metal atoms caused by momentum exchange from conducting electrons and defects, when the electrical field is applied. Since this is a form of diffusion phenomenon, the diffusivity of metal atoms are directly related to the EM property. For this, usually Cu doped Al has been used for slowing down the Al grain boundary diffusion, resulting in much better EM property. One problem here is that by adding Cu to Al, the resistivity becomes higher, and Cu doped Al has about twice larger resistivity than Cu. In fact, Cu has better electromigration and stress migration properties compared to conventional Cu doped Al metallization, which makes Cu interconnect more attractive.[76]

However, the implementation of Cu interconnects (or other noble metals including Ag and Au) with scaling raises new challenges in metallization technologies. In particular, dual damascene features (i.e, a trench with an embedded via), which are desired for Cu interconnect structures, require highly conformal, very thin film deposition for diffusion barriers and adhesion layers.[77] Additionally, Cu electrodeposition requires thin seed layers for nucleation and the initiation of plating. Currently, the conventional means of depositing these layers are I-PVD and

its derivatives. Compared to CVD or ALD thin films, PVD has benefits such that the deposited films are usually pure and wide range of materials can be deposited with little limitation. Nevertheless, any PVD based technology would suffer even more as the device scaling continues, primarily due to the poor conformality and thin sidewall coverage for a steep or high aspect ratio feature. The ALD process is intrinsically conformal and spatially uniform, and the films are often amorphous or poorly crystallized, which will help limit diffusion across the film barrier.

Other important applications for metal and nitride thin films grown by ALD in semiconductor device fabrication include gate materials for CMOS as well as electrodes of capacitors used in DRAM. Fig. 10 shows the potential applications of ALD metal/nitride thin films and candidate materials in CMOS device fabrications and more details for each application are described below.

1. Interconnect diffusion barrier/adhesion promoter

For all noble metals to be used as interconnect materials, thin diffusion barrier should be used between the metals and dielectrics, since the noble metals, including Cu, are fast diffuser into dielectrics as mentioned above. An additional function of diffusion barrier is as adhesion promoter for Cu and the interlayer dielectric. If the diffusion barrier materials do not adhere to the underlying layer or interconnect material, or if Cu does not adhere to the diffusion barrier, the result will be gross delamination and failure typically during the CMP steps used to planarize the deposit following plating. More importantly, bad adhesion causes severe reliability problem including EM.[78]

Thus, the basic material property requirements for Cu diffusion barriers include low solubility in Cu, low-to-moderate deposition temperature, low stress, good growth and adhesion on low k, etch stops, or SiO_2, and ideally good electromigration resistance when used in conjunction with Cu.[76,79-83] Several materials have been considered and studied as barrier materials for the Cu interconnect (Table 3.1). Among these, the transition metals and metal nitrides including Ta, TaN, TiN, W_2N, $TiSi_xN_y$, and $TaSi_xN_y$ have been the most promising candidates for diffusion barriers for Cu in modern devices.[82,84-86] For current Cu interconnect technology, TaN/Ta provides best results in terms of various factors including EM and via resistance, and process related issues.[82] As the device size shrinks below 100 nm node, the volume ratio between diffusion barrier materials and interconnect metal becomes significant.[9] In addition, the average thickness of diffusion barrier materials are limited by the increase in resistance.[76] So very thin, but functional diffusion barrier materials with excellent conformality and are desired. Considering these, ALD of metals/nitrides is a promising ultra thin diffusion barrier deposition technique.

2. Interconnect seed layer: Cu seed or direct plating materials

Electrodeposition or electroplating of Cu has evolved into the standard technique for the filling of the lines and vias used for the majority of the interconnect features in the current logic semiconductor devices. The process is inexpensive and techniques have been developed for "superfilling," or the filling of deep, high aspect ratio features from the bottom up.[87] By adding organic additives to Cu plating solution, the deposition rate on the surface is suppressed, and a higher deposition rate remains inside of the trenches, resulting in void free filling.[88] This differs from conventional CVD technology, which tends to fill features in from the sides, resulting in a

center seam. In addition, because the Cu grains in an electroplated Cu film (following annealing) are large, this results in a “bamboo” microstructure with grain boundaries mostly orthogonal to the current flow direction, resulting in better electromigration resistance. However, Cu cannot be easily electroplated on the refractory metals and nitrides used as diffusion barrier materials without an additional Cu seed layer. So far, Cu seed layer has been deposited mostly by PVD techniques for this purpose, primarily by various versions of I-PVD. However, with any PVD deposition technology, there is a slow build-out at the upper corners of trenches or vias, forming a slight overhang. In interconnect nodes above 130 nm or so, this overhang of perhaps 4-5 nm is not critical. However, as the interconnect nodes approach the 45nm node, this overhang (which does not scale down) will significantly close off the top opening of the via or trench, inhibiting the fill by electroplating. Therefore, a very conformal seed layer deposition technique will be required by that generation, and this may only be achievable by ALD.

Cu electrodeposition can be also done on other low-resistance conductors. The required material properties for this purpose include nobility, formation of soluble or conducting oxides, and insolubility in Cu. An ideal direct plating material should have good diffusion barrier properties as well as good adhesion to dielectrics. A few metal layers have been identified as candidates, which are mostly refractory metals such as Pd, Pt, Ru, Rh, Ir, Ag, Co, Mo, Cr, and W.[75,89] However, there has been little work published on the usage of these materials in interconnect structures, and significant additional work remains to determine whether any of these candidates are acceptable.

3. Contact, via plug and barrier

The "contact" is the electrical structure that makes connection between the Si-level device and the first level of the interconnect circuitry. Tungsten has been the most successful metal used for this purpose, and it has been deposited by means of a high step coverage CVD process using WF_6 as metal precursor.[62] Even with its relatively high resistivity (bulk = 5.7 μΩ cm, CVD W approx 2-3x higher), the contacts are short enough that the net resistance is minimal compared to the silicide and junction resistance. Instead, the material property which is more important for contact application is reliability issue including EM, which makes W the best choice to replace high resistivity poly-Si.

The application of CVD W for contact and plugs requires both an adhesion layer to oxide and more importantly a barrier layer to limit the interaction of WF_6 and Si or SiO_2 layers, since WF_6 is very reactive with Si, Al, or Ti.[7] For example, Si reacts with WF_6 forms volatile SiF_4, which would result in voids at the Si contact. This causes poor electrical contact and high junction leakage. CVD TiN films deposited by either a halogen (chloride) or MO source have been widely used for this purpose.[7] A layer of Ti is also needed under the TiN film to make better electrical contact at the bottom of the contact. However, due to the difficult nature of conventional Ti CVD (using halide plus hydrogen, for example), PVD Ti has been generally used.

The existing CVD W technology becomes limited at high aspect ratio due to poor nucleation and low rates. This is compounded by the poor scaling of the CVD TiN process as well as the PVD Ti contact layer. Each of these areas is an opportunity for improvement using ALD or hybrid-ALD/CVD technologies, which will scale well into these advanced generations. At least for nucleation level of W deposition it seems inevitable to use ALD techniques, which has become almost commercially available now.

4. Metal gate electrode

Another important application of metals and conductive nitrides is for device level structures, especially as electrode materials. With the continued CMOS scaling, the metal gate electrode has been widely studied due to the advantages compared to the conventional polysilicon gate electrode.[90] One of the biggest advantages is the removal of depletion effect, which accounts for 4-5 Å of equivalent oxide thickness in inversion during operation of the device. In addition, the B penetration (into the gate dielectric) from p-type poly Si gate is removed. With a metal gate, the high temperature activation process required for the poly Si gate can be removed, which has potential benefits in terms of concerns over the thermal instability of most of the potential high k gate dielectric materials.

For material properties point of view, the work function is the most important property of any replacement gate material. The workfunction of a metal gate should be within 0.2 eV from conduction or valence band edge of Si for p-FET or n-FET devices, respectively. In addition, the candidate metals should satisfy various aspects of gate materials, such as high thermal stability, low reactivity, and low electrical resistivity. The selection of the deposition technique for gate material is also critical. A damage free deposition technique is desirable, and as such, PVD is generally not considered a good technique. Also, the impurity level in the gate electrode must be very low, since any impurity introduction into gate stack could be detrimental for CMOS performance. Particularly, the use of metal gate with low level Cl (impurity) is critical to minimize the capacitance-equivalent thickness increase and prevent long-term reliability issues. To deal with many of these issues and constraints, ALD of the gate metal is a desirable direction to proceed.[71,91] Although the temperature limit for the gate electrode application is not as severe

as for the interconnect (BEOL) applications, a very high growth temperature is not desirable especially for the deposition of metal gate on high k materials, which tend to be less stable than conventional SiO_2 against metal films. In addition, the replacement gate technology shown in Fig. 11, which is one of the promising integration schemes for metal gate devices, requires deposition of metal films for nano-scale gate structures with high aspect ratio.[92] This makes ALD even more attractive. Table 3.2 shows some possible candidate materials for CMOS metal gate.

5. Electrode for DRAM technology

As dynamic random access memory (DRAM) cells also scale to increasingly smaller dimensions, new high k materials such as Ta_2O_5 and Al_2O_3 have been studied as novel dielectric materials for the metal insulator semiconductor (MIS) capacitor or metal insulator metal (MIM) capacitor. In addition, one of the key technologies in a MIS or MIM capacitor is the implementation of metal electrode, since the electrode resistivity could be reduced by replacing the current poly-Si structure with a higher conductivity metal electrode. For integration of high k materials with metal electrode, the selection of high k materials and metal electrode is far from trivial, since the deposition of high k materials require high growth temperature and the high k materials usually require thermal treatment at high temperature in O_2 environment.[93,94] Thus, the electrode should endure high temperature process and prevent oxygen migration, for which refractory metals including Pt, Pd, Ir, and Ru are considered as promising candidates. For MIM stack capacitor, Ru or Ir has another benefits since they have low resistivity oxide and the dielectric constant of Ta_2O_5 deposited on these materials is higher (up to 50).[95] Thus, a number of studies have been reported on Ru CVD using various precursors recently.[96-98] But for very

high aspect ratio structure, ALD may be the only viable technique available. Additionally, for MIM structure, liner material such as TiN is required, preventing reaction between Si and electrode metals, which also can be deposited by ALD. Meanwhile, for current trench DRAM integration schemes, it is required that the node dielectric and metal electrode endure the front end processing thermal budget of up to 1050 ºC, and TiN is one of widely studied material as a thermally stable metal electrode material for this application.[99,100] Since ALD has the ability to produce TiN films at lower temperature with very low Cl impurity levels, TiN ALD is a promising process.[99] Moreover, the aspect ratio of the DRAM trench capacitor has extremely high aspect ratio up to 60:1, which requires very good conformality. ALD TiN can satisfy this need, as shown in Fig. 12.[100]

6. Other applications

In addition to the applications mentioned above, ALD of metal and nitride thin films could play a role in many novel structures and applications. For example, in the emerging field of nanotechnology, ALD is attractive nano film deposition technique because of the intrinsic control over the deposition thickness, even at below the monolayer level. Several applications of ALD in nanotechnology have been discussed in an earlier report.[12] Recently, TaN ALD film was used as electrode materials for high storage capacitor structure (at the sub-20 nm scale) prepared by self-assembled nanostructures using copolymer diblock process.[53] Also, Ru ALD process has been used for making RuO_2 nano tubes using carbon nanotube template, showing the potential of ALD for nanotechnology area. Fig. 13 shows the TEM images of Ru nano films deposited inside and outside of carbon nanotubes.[101]

IV. Characterizations of ALD metal/nitride process and film properties

Various analysis techniques have been used to analyze properties of ALD metal and nitride films. For *ex-situ* measurements, conventional thin film analysis techniques including TEM, x-ray diffraction (XRD), Rutherford back scattering (RBS), second ion mass spectrometry (SIMS), Auger electron spectroscopy (AES), x-ray photon spectroscopy (XPS), and energy dispersed x-ray (EDX) have been employed for microstructural and chemical analysis. For *in situ* analysis, however, several techniques unique to ALD have been performed. Typically, since the process pressure during the ALD is not in an UHV condition, *in situ* analysis techniques such as low energy electron diffraction (LEED), reflection high energy electron diffraction (RHEED), or AES, which are common tools for molecular beam epitaxy (MBE) or gas-source MBE, are difficult to be used. Table 4.1 summarizes the analysis techniques reported for metal and nitride thin films.

1. The *ex-situ* analysis techniques and film properties of ALD films

1.1 Film thickness; growth rate and density

In contrast to the other deposition techniques, such as CVD or PVD for which the growth rate is represented by thickness per unit time, the growth rate for ALD is usually represented by the deposited thickness per cycle. Thus, the growth rate is usually determined by measuring the film thickness divided by the total number of cycles. Various *ex situ* analysis techniques have been used for thickness measurement; cross-sectional measurements using TEM and scanning electron microscopy (SEM) images as well as spectroscopic methods such as RBS. In addition, conventional XRD or special X-ray technique such as x-ray reflectivity (XRR) have been used. Depending on the measurement techniques used, the apparent thickness may be different due to

the non-ideal density of the grown films. For example, while RBS gives the total number of atoms in the film, the physical thickness is obtained by microscopic techniques. By comparing these values, a functional film density is calculated. The film density of MO ALD nitride films is generally lower than that from halide sources.

For ideal ALD, since the thickness increases linearly with increasing number of cycles, the thickness divided by number of cycles should always give same value irrespective of the total number of cycles. However, the growth rates are frequently different for initial deposition cycles compared to the later deposition cycles. One of the most common reasons for this is the problem in nucleation process. A classic example of this is observed for W ALD using WF_6 and Si_2H_6 on SiO_2 substrate.[102] In this case, up to 10 cycles of nucleation cycles was needed before linear increase in thickness as shown in Fig. 14, where the thickness was measured by *in situ* AES. This initial slow deposition was attributed to the very low sticking probability of the precursor on SiO_2 surfaces, where the surface hydroxyl groups play a role as adsorption sites. Thus, the smaller reaction site density results in smaller growth rate until fraction of initial substrate material is covered by deposited film. More recently, similar slower initial deposition rates for up to 40 cycles has been reported for TiN ALD.[103] In addition, the saturation coverage or reaction chemistry difference between substrate materials could produce a non-linearity for initial cycles, resulting in either an initial delay in deposition or a faster initial deposition rate for the first few cycles as observed for PE-ALD of Ti.[22]

1.2. Composition and impurity content

The incorporation of contaminants from precursors, for example the halogen from halide sources or carbon from metal organic sources, is a critical problem for the application of the

ALD films. Thus, the chemical analysis for the ALD films is essential and common chemical analysis techniques such as AES, XPS, RBS, and EDX are used for this purpose. Among these various techniques, RBS is an intrinsically quantitative technique.

The halogen content in ALD-grown films is significantly lower compared to that of CVD films using same precursors at the comparable growth temperature. For example, for TiN deposition with $TiCl_4$ and NH_3, the Cl content for a CVD TiN film grown at 500 ºC is 2-4 %, while for ALD TiN film at only 400 ºC, the Cl level is usually near 0.5 %. The carbon incorporation for MO ALD is almost inevitable from the organic ligands. For example, the carbon content in MO ALD TaN has been reported as high as 15 %.[45]

For transition metal and nitride ALD films such as TiN and TaN, the incorporation of oxygen can often occur by post deposition air exposure.[16,27] For further examination of this situation, a surface-specific technique such as medium energy ion spectroscopy (MEIS) has been used.[53] For the oxygen contamination by post deposition air exposure, the O containing layer is expected to be located only at the top surface, as was observed with halogen-based PE-ALD TaN.[53] However, a comparable study on halogen-based TiN ALD using RBS has shown that O is evenly distributed through the film.[16] This was attributed to the diffusion of oxygen, which was incorporated by post deposition oxidation, through the deposited film.[16]

PE-ALD usually incorporates H atoms in the film.[44,45] To measure hydrogen composition in the film, nuclear reaction analysis (NRA) or forward recoil elastic spectrometry is used. In addition, another major chemical analysis for nitride ALD films is the composition ratio between metal and nitrogen. This is usually determined by RBS or AES, but the AES has a problem in determining absolute nitrogen content in the films due to the matrix effect.

1.3 microstructure, roughness

XRD is the most common technique to determine the phase information and microstructure of the ALD film. Conventional XRD does not provide detailed microstructural information, which can be obtained by TEM or focused ion beam (FIB). For example, high resolution TEM (HR-TEM) can determine the existence of nano-size grains with very small portion in amorphous matrix. Due to the low growth temperature during ALD and absence of significant kinetic energy as in PVD, amorphous films are often obtained for ALD.

Ideally, a film deposited by ALD is expected to be very flat, since the growth occurs in a layer-by-layer manner. In reality, however, very rough surface is often obtained. The most common reasons include the limited adsorption/nucleation sites and concurrent etching during the deposition. For roughness measurements, AFM is the most widely used technique, which routinely give quantitative root mean square (RMS) roughness value with microscopic morphology. In addition, other techniques such as XRR can give more information on interface roughness. The interface quality is especially important when the ALD metal layer is used for gate electrode. XRR has benefit of yielding interface and surface roughness at the same time.

1.4. Conformality, uniformity

The most common technique for determining conformality is cross sectional electron microscopy such as SEM and TEM. While SEM has limitation for very thin films due to lower resolution, cross sectional TEM is often the only technique to determine the conformality for nanometer-scale layers. The conformality is usually represented by the ratio between thickness on the trench or via bottom or sidewall and that on the planar wafer surface after depositing the film on high aspect ratio structure. As mentioned above, ALD inherently produces films with

good step coverage. However, several factors could affect the overall conformality. The recent study has shown that high enough exposure of precursor is very important for good conformality film deposition by ALD.[104] In addition, other factors leading to CVD-like reactions such as insufficient purging or improper growth temperature result in poor step coverage. For PE-ALD, the recombination of reactive species (atomic hydrogen, for example) on chamber walls or even on the sidewalls of deep, high aspect ratio features could also be important factor.

1.5. Electrical properties

The most widely measured electrical property for metal or conducting nitride films is electrical resistivity. For this purpose, a four-point probe is used to measure sheet resistance (R_s) and the resistivity is obtained together with thickness measurements based upon $\rho = R_s t$. Thin films often have a higher resistivity than bulk, and the resistivity is a function of various factors such as film composition, impurity content, and density. In addition, if thin metal film is deposited in a metastable phase, a much higher resistivity is often observed. For example, Ta films deposited by PVD are often the beta (tetragonal) phase depending on the substrate materials and deposition conditions, and the electrical resistivity of this phase is nearly an order of magnitude larger than the alpha (bcc) phase.

The deposition of Ta using PE-ALD with a tantalum chloride precursor with atomic hydrogen resulted in amorphous Ta with similar resistivity to that of with beta phase.[27] In addition, for both PE-ALD Ta and TaN, the films have shown increase in sheet resistance with air exposure time, which was attributed to the surface region oxidation.[27] Another aspect of resistivity in nanoscale device era is the thickness effect on resistivity; the so-called ‘size effect’. Due to electron-surface scattering, the resistivity of Cu and diffusion barrier layers increases with

decreasing thickness for nano-scale thickness.[9] The presence of grain boundary and surface roughness also contribute to increase resistivity. Fig. 15 shows the calculated results of increase in Cu resistivity as the line width decreases, indicating that this effect could impose significant problems in sub-100 nm technology node.

In nanoscale device, since the diffusion barrier thickness will be very small, the resistivity constraint of the materials is released because the via resistance, rather than resistivity itself, is more important for device performance. For example, the sidewall thickness of PVD Ta or TaN, which is the most widely used Cu diffusion barrier material currently, is much thinner than that of bottom of the vias or trenches. For this case, to provide enough sidewall coverage, thicker materials than needed are deposited. This extra diffusion barrier material produces high via resistance. Thus, if ALD diffusion barrier with higher conformality is employed, higher resistivity materials can be used, which has effectively smaller via resistance. For example, recent study has shown that ALD WC_xN_y barrier with higher resistivity than PVD Ta (600 – 900 vs 15-20 μΩcm) was measured to have lower via resistance for 9K via chains with 0.25 μm vias.[105]

For gate electrodes, the work function is a key electrical property. When there is no charge present in the oxide or at the oxide-semiconductor interface, the flat band voltage simply equals the difference between the gate metal workfunction, Φ_M, and the semiconductor workfunction, Φ_S. However, the charge in the oxide or at the interface changes this flatband voltage. When interface charge Q_i presents at the interface between the oxide and the semiconductor[106]

$$V_{FB} = \Phi_{MS} - Q_i/C_{ox} = \Phi_{MS} - t_{ox}Q_i/\varepsilon_{ox} \quad (6)$$

where C_{ox} is the capacitance, t_{ox} is the thickness, and the ε_{ox} is the dielectric constant of the gate oxide, respectively. And the second term (Q_i/C_{ox}) corresponds to the voltage across the oxide due to the charge at the oxide-semiconductor interface. After the flat band voltage (V_{FB}) is measured as a function of oxide thickness on a device or dot capacitance structure, which is fabricated from the metal thin film deposited on oxide layer, the workfunction (Φ_{MS}) and interface charge (Q_i) are determined according to eq. 6. However, the exact workfunction determination is not always trivial and the workfunction of ALD deposited metal or nitride thin films has been rarely reported. There are other indirect methods to determine workfunction such as photoemission spectroscopy.[106]

1.6. Diffusion barrier properties

To evaluate the ability of an interconnect diffusion barrier to withstand either the diffusion of Cu from a line or via, or the diffusion of contaminants into the Cu from the ILD, it has been generally necessary to construct test structures which are then subject to either elevated temperature, an applied electric field, or both. The simplest test structures consist of a Cu film deposited over a diffusion barrier, which is deposited onto clean Si. A schematic drawing of sample test structure for ALD Ta or TaN is shown in Fig 16a. The samples are annealed in various gas environment such as N_2, He, Ar or in vacuum. When Cu is deposited right on the HF cleaned Si substrates (i.e., Si without native oxide), Cu reacts readily with Si at about 260 °C without diffusion barrier.[53] But with the presence of a barrier the reaction (or barrier failure) occurs at much higher temperature. Since Cu_3Si is formed for Si substrates after Cu indiffusion through the barrier caused by annealing, XRD is widely used to determine diffusion barrier failure for diffusion barrier on Si substrate by detecting the formation of the silicide phase. Also,

the elimination of the metallic Cu phase measured by the Cu XRD peaks intensity decrease is another indication of Cu indiffusion. Usually, the test structures are annealed at various temperatures and XRD spectra are obtained to determine the failure temperature. In parallel, changes in other physical properties caused by diffusion barrier failure can be used. For example, due to the disappearance of top Cu layer and reaction with substrates at failure temperature, abrupt sheet resistance and surface roughness increases are observed.[27] Recently, *in situ* diffusion barrier failure temperature measurements during controlled heating of the sample, using synchrotron XRD, combined with four point probe measurement and optical scattering, have been applied to analyze ALD Ta thin films as Cu diffusion barrier.[27] Fig. 16b-d show that the failure temperature of PE-ALD Ta film with 7 nm thickness is around 730 ºC. At this temperature, the formation of Cu silicide is observed in XRD intensity contour map (Fig 16b), accompanied by the rapid increase of optical scattering intensity (Fig 16c) and resistivity (Fig 16d).

An etch-pit test is another widely used diffusion barrier test method for diffusion barrier on Si substrate. For this, Cu deposited on barrier material on top of Si is selectively etched with an acid after annealing, and the formation of any etch pits is observed by microscopy. For example, diluted NH_3 for Cu and NH_4OH/H_2O_2 mixture for TiN are used for etching. Finally, Si surface is etched by Secco etch solution (Mixture of K_2Cr_2O7:H_2 and HF = 1:1). By observing the formation of etch pits on the Si surface it is determined if there has been reaction between diffused Cu and Si.[107] The etch-pit test gives a lower failure temperature than the XRD or resistance measurements.

For detecting the Cu diffusion to other substrate materials such as SiO_2 and low-k materials, chemical analysis techniques are used. Chemical composition measurements such as

RBS, XPS, AES, or SIMS have been employed, and depth profile of Cu before and after annealing shows the diffusion profile of Cu into substrates.

For determining the diffusion barrier property in a near-operating condition, an electrical test for a device structure is used. The simplest method is the measurement of the change in capacitance-voltage curve for test structure, typically Cu and barrier films deposited on dielectric materials.[108] In a previous report on ALD TiN, C-V measurements were performed on MOS capacitor structures formed on thin SiO_2 layer, before and after annealing. Since Cu atoms form deep donor levels in Si and act as the generation and recombination centers, the low frequency-like C-V characteristic is observed for high frequency condition when Cu diffusion through TiN diffusion barrier has occurred. A more common and sensitive test is a stress-induced diffusion test such as bias temperature stressing (BTS). Here, after high bias is applied to the MOS structure at moderate temperature (200-300 °C), the flat band voltage shift in capacitance-voltage curve is obtained.[106] From the voltage shift, the mobile charge (the amount of diffused Cu ions for Cu diffusion barrier measurement) is determined. This technique was employed for measuring the Cu diffusion through ALD TiN layer.[17] Another variation of the technique includes triangular voltage sweep (TVS), where the current is measured instead of capacitance.[106] The measurement techniques for diffusion barrier studies of ALD films are summarized in Table 4.3.

1.7. Other properties

There are several other important properties of ALD films for BEOL applications. One of the key issues is the adhesion between deposited ALD films and substrate materials or capping layer. The simplest, generic test is the Scotch tape test, which is performed by pulling the

adhesive tape from the deposited surface. For a more quantitative measurement, however, a four point bending test has been used.[109] In this case, the adhesion is quantified in terms of the force. Little result has been reported for the ALD metals or nitrides thin films using this test, but the PE-ALD TaN film has shown similar adhesion strength compared to PVD TaN.[110]

Another key factors for the evaluation of diffusion barrier materials in Cu interconnects features are electromigration resistance and stress migration resistance among other reliability issues. These reliability failures are typically characterized either by an increase in line resistance or by a line becoming an open circuit, usually in terms of median time to failure (MTTF). [106] To decrease the measuring time, measurements are done at higher temperatures or increased current density. For reliable statistical data, a large number of test lines or structures should be tested. Recently, the reliability of ALD TaN diffusion barrier was investigated, showing comparable results to PVD TaN.[111]

2. *In situ* characterization of ALD process

ALD occurs through layer-by-layer surface reactions and the amount of deposited films per cycle is typically in the submonolayer range. Thus, submonolayer resolution is required to monitor the reactions *in situ.* In addition, since ALD has a relatively high working pressure compared to other UHV-deposition techniques such as MBE or UHV-CVD, there is a limitation in the use of various surface analysis techniques. Table 4.3 summarizes the *in situ* reaction monitoring techniques applied for metal/nitride ALD processes.

Quartz crystal microbalance (QCM) is one of the most widely employed processing monitoring techniques for ALD.[112,113] QCM has been used widely for the thickness calibration of evaporation or sputter deposition. The principle behind this technique is the resonant

frequency changes of a quartz crystal due to small change in mass caused by the deposition of a film on the surface of the crystal. The mass change, which can be directly converted to thickness of deposited film (assuming a known density), is linearly related to the mass change as,[113]

$$\Delta f = -C\Delta m$$

where C is the crystal-dependent constant which incorporates the shear modulus and density of the quartz crystal. The resolution of the technique is dependent on mainly on the ability to measure small frequency changes at the operating frequency of about 6 MHz. Recent versions of these systems can easily resolve 0.1 ML, which is adequate for observing and diagnosing ALD processes.

By using QCM, the thickness data can be plotted as a function of time during each of the 4 steps of the ALD process. As an example, the QCM signal vs reaction step for Al_2O_3 ALD from TMA and H_2O has been shown in Fig. 17.[112] (Here, the oxide ALD has been shown as an example, but the similar results are obtained for metal or nitride ALD) The initial adsorption of the metal precursor (TMA) is easily observed, along with the self-saturation nature of the deposition (step 1). The reaction step (3) is also easily observed by a mass change on the microbalance crystal, due to the release of volatile byproducts and formation of oxide from the reaction. The net increase at the end of each cycle corresponds to the deposited film thickness per cycle on the surface. With suitable calibration (and knowledge of the functional area of the crystal), this mass increase can be converted into a ML/cycle value. This technique is invaluable as a means of diagnosing the individual process steps of the ALD sequence, and has been used widely to both characterize the deposition process as well as to understand the reaction kinetics. QCM has been employed many times for oxide ALD,[112-116] but has been rarely used for

metals/nitrides ALD. Recently, QCM was used for Ti PE-ALD for investigating growth kinetics and related surface chemistry.[22,40]

One limitation of this technique is that the deposition should be performed on quartz crystal, as opposed to a measurement on a wafer surface. However, by pre-deposition of various materials on the quartz crystal, the growth on different substrate materials has been studied.[22,39] Another problem with this technique is that the measurement is quite dependent on the temperature, as demonstrated recently.[48] Thus, properly calibrated profile is needed for real data measurements, to compensate the temperature effect.[113]

As an alternative *in situ* thickness measurement, spectroscopic ellipsometer has been employed for W and W_2N ALD.[117] In this case, the optical thickness changes, rather than the real mass increase of deposited thin films, are obtained. While the strong point of this technique is that the deposition on real substrate is monitored, the difficulty is that the dielectric or optical properties of many materials is unknown.

While the QCM or ellipsometry measures the change in film thickness without the ability to detect the reactive species, a mass spectrometer provides the information on the produced chemical species during reaction, which is essential to study the reaction mechanisms. However, as mentioned above, ALD usually occurs at high pressure, from mTorr to Torr, and a differential pumping system is required for implementing *in situ* analysis using mass spectrometer.[118,119] The partial pressure of the reactive species and byproducts are obtained as a function of process time while the precursor pulses are introduced sequentially into the chamber. Mass spectrometer analysis is a powerful technique to observe the byproduct directly, but if the reaction involves various species or chemically complicated precursors are used, it is difficult to distinguish all the species. For example, when the precursors contain organic ligands, the spectra include various

combinations of hydrocarbons, which makes the identification of each chemical species difficult. Only recently, a study on TiN and $TiAl_xN_y$ ALD using *in situ* mass spectrometry has been reported.[23] In this study, to enhance the selectivity of reacting species and byproduct, ND_3 was used instead of NH_3. For TiN ALD using $TiCl_4$ and ND_3, DCl was detected as the only byproduct, and the DCl signal was obtained as a function of time.[23] (Fig. 18) From the intensity of the DCl signal, the relative flux of DCl was obtained, from which the information on the reaction mechanism has been obtained.

In addition, various *in-situ* surface analysis techniques, including Fourier transform infrared (FTIR) spectroscopy, AES, and XPS, are direct measurement of surface species deposited at each reaction step. These techniques are generally incompatible with an ALD deposition chamber, so it is necessary to transport the sample under vacuum from the ALD part of the system to the analysis chamber. George et al. studied the W and W_2N ALD process by FTIR.[25,117,120] One benefit of FTIR is that it can distinguish various modes of chemical bonds on the surfaces, which enables the detailed study of the chemical pathway. However, conventional substrates cannot be used for FTIR spectroscopy due to the small signal level. A special substrate with much higher surface area such as powder or beveled substrate with multiple internal reflections is required for thin film study. For W and W_2N ALD study, silica powder was used as the substrate to obtain a large enough surface area. Alternately, surface composition measurement such as XPS and AES were employed for W ALD.[102,121] With the inherent high sensitivity of these techniques, the nucleation process during initial several cycles has been investigated. Recently, a real time measurement of resistivity using a four point probe has been reported for W ALD.[123] The resistivity was measured continuously during the alternate WF_6

and Si_2H_6 exposure as shown in Fig. 19. This kind of *in situ* novel analysis technique is expected to provide more insights in understanding ALD processes.

V. The current research status of metal or nitride ALD

1. Titanium and titanium nitride

TiN has drawn extensive attention for several key areas in semiconductor device process including diffusion barrier, conducting electrode, and antireflection coating layer in the interconnect stack, due to its good thermal and mechanical properties and low resistivity. Among them, application as a diffusion barrier for W plugs has been extensively studied and numerous CVD and PVD tools are widely available. ALD of TiN has been one of the most widely studied nitride ALD processes, partly due to the availability of good precursors in both the halogen and MO realms. $TiCl_4$ is one of the rare liquid halide precursors, and has large vapor pressure even at room temperature. However, the deposition of Ti or TiN by CVD using $TiCl_4$ and or H_2 or N_2/H_2 requires high growth temperatures usually above 750 °C.[62] Although TiN CVD has been reported to occur at as low temperature as 550 °C using $TiCl_4$ with NH_3, this is still much higher than the maximum allowed temperature (400 ºC) in interconnect processing. This has led to the development of MO CVD TiN processes, using, for example, TDMAT and NH_3, which can be operated at <400 ºC, and has been widely adopted for current semiconductor device fabrication.[7] However, due to the low resultant film density and high carbon and oxygen content, additional plasma treatment on the deposited film is usually performed.[124]

1.1 Ti ALD

The only Ti ALD reported so far was by PE-ALD using halide precursors.[22,39,43] Ti films were grown by using $TiCl_4$ and atomic hydrogen generated by rf plasma at growth temperatures below 300 °C. Recently, the growth kinetics during PE-ALD Ti were studied by QCM as a function of various key growth parameters.[22] The key kinetic parameters for Cl extraction reaction and $TiCl_4$ adsorption kinetics were obtained and the growth kinetics were modeled to predict the growth rates. In addition, the dependency of growth kinetics on different substrate materials was investigated during the early stages of deposition with various thin films predeposited on the crystal rate monitor surface by sputtering or evaporation. However, the deposited ALD Ti was quite unstable to air exposure. ALD Ti films were observed to oxidize within a few seconds upon removal from the ALD chamber and exposure to the air. Thus, ALD Ti process, which can be readily used as practical application, is not available yet.

1.2. TiN ALD process

The first TiN ALD using $TiCl_4$ and NH_3 was reported over 15 years ago,[14] but more systematic study of TiN ALD has not begun until recently by Ritala et al.[16] Though the cubic TiN phase with resistivity of 250 μΩcm has been deposited by thermal ALD, low Cl content below 0.5 % was only achieved above a 500 °C of deposition temperature. As an effort to decrease deposition temperature, an additional reducing agent Zn, was used. In this case, the resistivity as low as 50 μΩcm has been achieved.[16] The deposition rate was quite low (0.2 Å/cycle), but the deposited TiN has excellent step overage.[125] More detailed characterization of the effect of Zn was investigated using various analysis techniques.[126] The main reason for improvement of resistivity for the process using Zn was found due to decreased O content (2% with Zn vs 15% without Zn) rather than changes in Cl content. With decreased O contamination,

Hall measurements indicated that the effective carrier density and mobility of ALD TiN have shown enhancement. However, the use of Zn has limitation in the application for semiconductor device processing and the Cl content using the Zn reduction enhancement at 400 °C was still high.

To obtain lower Cl content film at low growth temperature, other non-metal reactants have been tried. DMHy was used as alternative nitrogen source/reducing agent.[67] Although cubic TiN has been grown at as low temperature as 250 °C, the C and O content was higher than NH_3 process, which resulted in higher resistivity. In addition, the Cl content was higher than 2% even at 500 °C. Another reducing agent, TMA has been tried, but $TiAl_xN_y$ instead of TiN has been deposited due to the incorporation of Al from TMA.[52] In this case, however, the O content was quite low, which was attributed to the thin Al oxide layer formation. Additionally, by using other alternative nitrogen source, such as tertbutylamine and allylamine, gold colored TiN films with relatively bw resistivity were obtained.[127] In contrast to DMHy, little C was incorporated for tertbutylamine, which was attributed to the weakly bound tertbutyl group, enabling easy β-hydrogen elimination. For both cases, amorphous films were grown, which might be useful for diffusion barrier applications. Jeon et al. also used $TiCl_4$ and NH_3 for ALD TiN, and studied the dependence of ALD TiN properties on different Si substrate orientation. For this case, low resistivity film was deposited at low growth temperature as low as 350 °C, with Cl content below 3%.[15,128] Little difference was observed in terms of microstructure, growth rate, and density depending on Si substrate orientation.

In a recent report, much slower growth rate was observed for early stage of growth (<50 cycles) on thermal and PE-CVD silicon oxide surface.[103] At the same report, Ti surface coverage determined by low energy ion spectroscopy (LEIS) has shown that only 55 % of oxide

surface is covered by TiN up to TiN thickness corresponding to $2x10^{15}$ Ti/cm^2, indicating that TiN islands are grown vertically before the oxide surface is covered completely by TiN layer. At higher growth temperature, the thickness of TiN needed to fully cover the oxide surface decreased (about 25 Å at 400 ºC), with higher uniformity.

As an effort to grow lower resistivity films at low temperature without Zn, TiI_4 was tried as the Ti precursor.[129] This idea was based upon the lower Ti-I bond energy (- 296 kJ/mol) compared to that of Ti-Cl (- 429 kJ/mol).[130] As an additional benefit, the residual I in TiN film would cause less potential problem in Si device process than Cl, since I is much heavier than Cl, requiring higher thermal energy for outdiffusion from TiN lattice.[130] The growth rate was found to be lower compared to $TiCl_4$ case (0.13 vs. 0.17 Å/cycle at 400 °C), probably due to the larger steric hindrance due to the larger size of iodine ligands. However, in contrast to $TiCl_4$ process, the growth rate during TiI_4 ALD process increases continuously above 400 °C to as high as 0.3 Å/cycle at 500 °C. (Fig. 20) This was attributed to the partial decomposition of TiI_4 to TiI_x (X<4), probably caused by the smaller bonding strength between Ti-I. The low resistivity film below 100 μΩcm was obtained at above 475 °C of growth temperature.

Thus, the studies so far indicate that the thermal (i.e., non-plasma enhanced) ALD TiN using halide sources requires growth temperatures greater than 400 °C for satisfactorily low Cl content film. While this puts limitation for TiN ALD as interconnect applications, it is still an improvement compared to the CVD counterpart. Moreover, the main applications of TiN ALD are as electrode for DRAM capacitor and barrier for W plug, for which the growth temperature restriction is not so severe compared to Cu barrier applications.

ALD using metal organic precursors, TEMAT[54] and TDMAT[55,56,131], reacted with NH_3, were also studied for TiN ALD. In these cases, amorphous TiN was deposited at growth

temperatures around 200 °C. For both precursors, the self-saturation was not met at higher growth temperature above 220 - 230 °C, where the growth rate increases continuously with increasing metal precursor exposure. This indicates that the CVD type of growth occurs at this temperature range caused by thermal decomposition of the metal precursors. Also, in contrast to ALD using a chloride source, the thickness/cycle at the saturation condition was quite large, 4-6 Å/cycle, which is close to 2 ML rather than ideal 1ML/cyce.[54,55] To explain these results, a "readsorption" concept was suggested.[56,132] In this model, the MO sources adsorb on preadsorbed NH_3 molecules to form TiN instantly and additional adsorption of MO source occurs on the newly formed TiN surface. A similar concept has been applied for GaAs ALD.[133] The step coverage of MO-ALD TiN was about 98 % for 1:1 aspect ratio trench structure.[54]

There have been a couple of reports to deposit TiN thin films by PE-ALD. One recent report on TiN PE-ALD using $TiCl_4$ and H_2/N_2plasma has shown that TiN films with low resistivity of 80 μΩcm has been obtained with growth rate of 0.46 Å/cycle at 350 °C.[134,135] The Cl content of PE-ALD TiN was lower than 0.5 %, indicating better materials property compared to thermal ALD using $TiCl_4$ precursor. More recently, TDMAT and N_2, H_2, or N_2/H_2 plasma have been used for PE-ALD of TiN.[70] The TiN thin films, with lower than 4% of C and O contamination and 300 μΩcm resistivity, were deposited for N_2 plasma case, with good conformality. The growth rate was constant between 200 – 300 ºC, while it increased above 300 ºC due to the dissociation of metal organic source. For H_2 or H_2/N_2 plasmas, the C and O content were higher with higher resistivity. (for example, C > 16 % for H_2 plasma)

1.3. Material properties of ALD TiN

Overall, the properties of ALD TiN are superior to those of CVD TiN in terms of impurity content, density, and resistivity in addition to the obvious benefits of lower growth temperature and excellent step coverage. While the Cl content in ALD TiN is usually lower than that in CVD TiN for chloride based processes, the carbon content and resistivity are lower for ALD process than CVD for MO-ALD TiN.[57] This is probably due to the absence of gas phase reactions and the reaction between precursors has better chance to be completed during ALD. Another study on comparison between ALD and I-PVD TiN reported that the resistivity of ALD TiN films did not increase with decreasing thickness to 7 nm, but I-PVD TiN did increase over the same range.[17] This might be due to the smooth and uniform surface of ALD TiN film, resulting in smaller surface scattering at very small thickness.

The impurity content of ALD TiN is a strong function of growth temperature. For ALD process using $TiCl_4$, Cl contamination is one of the big issues, since Cl residue can cause problem in device performance, especially for reliability related problem. Generally, a Cl content below 1% is required for device fabrication. The removal of Cl requires thermal energy for HCl formation and desorption during NH_3 exposure, thus at low growth temperature Cl content becomes higher. Additionally, an increased concentration of NH_4Cl on the surface and a low Cl desorption rate at low growth temperature were suggested for the observed high Cl content.[19,128] Meanwhile, for the MO-ALD TiN, high carbon contamination is a significant problem, and is often above 10 %.[57] Until now, carbon free TiN MO-ALD has not been reported.

The resistivity of ALD TiN films also shows strong dependence on growth temperature, with higher values at low growth temperature. The primary reason is the high impurity content at low growth temperature, but the low film density may also contribute. Alternatively, the preferred orientation difference of deposited films was also suggested as the main reason.[18]

The oxygen contents of ALD TiN films have been reported to be high for most cases. Ritala et al. suggested that the oxygen is incorporated by post-deposition air exposure, based upon the observation that the O content in the film is higher for small thickness (32 % for 340 Å) while decreases for thick film (3% for 1400 Å).[16] In other study, O content was measured as highest at surface region, which strongly supports that the O is incorporated by post deposition air exposure.[107] For MO-ALD TiN films, large increase in oxygen content with air exposure time was reported.[57] After 30 days exposure, the O content increases from 20 to 30-40 % with increase in resistivity, which is known as aging effect. Post deposition rapid thermal nitridation (RTN) and plasma treatment for MO-ALD TiN was also investigated in this study. After RTN, C content decreased without changing in surface nitrogen content. The resistivity of the plasma treated TiN film remained same with air exposure, which was attributed to more dense, nitrogen rich surface formation.

1.4. ALD TiN: Diffusion barrier properties and other device related issues

For ALD TiN from halide precursors, the effect of different halogen precursors of TiN ALD on the Cu diffusion barrier property was investigated.[136] For three different combinations, $TiCl_4$+NH_3, TiI_4+NH_3, and $TiCl_4$+NH_3+Zn, little difference in Cu diffusion barrier failure was observed among them with only minor improvement for $TiCl_4$+Zn+NH_3 case. All ALD TiN films have shown comparable diffusion barrier failure temperatures to those of CVD and PVD TiN. In contrast, another report on barrier performance measured by the BTS technique has shown that ALD TiN has better diffusion barrier properties than PVD TiN.[17] In a more recent report for TiN ALD using $TiCl_4$ precursor, Cu diffusion barrier failure temperature of around 500 °C was observed by an etch test, which was comparable to CVD TiN.[107] Since ALD TiN

had significantly lower Cl content than CVD TiN using the same precursors, it was suggested that the Cl content does not produce much difference in diffusion barrier property. Rather, the similar failure temperature was attributed to the same microstructure between the TiN films deposited by ALD and CVD.

The post annealing effect on diffusion barrier property of amorphous ALD TiN films grown by MO-ALD was investigated using XRD and resistivity measurements.[58] MO-ALD TiN films (deposited between Cu and Si) prevented the formation of Cu silicide up to 600 °C, but a large increase in resistivity and Cu_3Si formation was observed for annealing at 650 °C, although TiN film did not crystallize up to this temperature range. Additionally, pre-annealing did not produce any significant change in the diffusion barrier property. Often, the decrease in resistivity with low temperature annealing for Cu/TiN/substrate structures has been observed, which was explained by densification of Cu or grain growth.[58,136]

TiN is one of the good candidates as gate electrode for CMOS or electrode for DRAM structures due to the good thermal and chemical stability and low resistivity. Park et al. investigated the application of ALD TiN as a metal gate electrode for CMOS and compared the electrical characteristics to PVD and CVD TiN.[71,91] Damage free TiN metal gate with low interface defect density (D_{it}) was formed on SiO_2 and high k with good reliability. The D_{it} value of ALD TiN was comparable to that of poly Si gate. In addition, the leakage current of ALD TiN was 2-3 times lower than that of PVD TiN. A similar comparative study has been performed for a TiN top electrode for Ta_2O_5 and Al_2O_3 MIS capacitors for DRAM application.[137] From electrical measurements of constructed MIS structures with CVD and ALD TiN electrodes, the leakage current was found to be strong function of step coverage, while the MTTF of TiN metal gate on high k gate oxide was determined mainly by Cl content. Both the leakage current and

MTTF were found to become worse with increasing growth temperature, which was attributed to the reduction of high k materials by NH_3 at elevated growth temperature. Since the process temperature of ALD TiN is at least a 100-200 °C lower than that of CV TiN, ALD has been suggested as a more promising technique for this application.

As an effort to investigate the integration of ALD TiN for Al interconnect applications, MO CVD of Al was grown on ALD TiN and reflectance spectroscopy was used to show that the thin ALD TiN layer (1nm) could produce much smoother Al film deposition by providing nucleation sites for Al CVD.[138,139] For Cu interconnects, the incompatibility of chloride chemistry on Cu was suggested as a potential problem for halogen-based TiN ALD.[105,140] Considerable pitting has been observed during TiN ALD on Cu, which was attributed to the formation of a volatile CuCl product or reduction of Cu oxide by chloride. This was less significant at low growth temperature below 300 °C. For comparison, W_2N ALD using fluoride source did not show the pitting on Cu surface.

Another important issue for device fabrication is the ALD of TiN on low k materials. TiN ALD from $TiCl_4$ and NH_3 on Si-C-O and amorphous SiC:H films and the effects of O_2-based plasma treatment were studied.[103,141] Since the number of reactive sites on low k is small (compared to silicon dioxide) and the distribution is inhomogeneous, ALD could be more problematic on low k materials. The TiN ALD films on Si-C-O surface were not continuous and had high resistivity, which was attributed to the small number and uneven distribution of reactive sites on low k materials. After O_2/N_2 plasma treatment of the surface, continuous films with lower resistivity were grown. SiO_2-like thin layer formation on Si-C-O films after C elimination by plasma exposure was suggested as the reason, based upon the low C content observed after plasma treatment. In contrast, continuous TiN films were deposited by ALD on SiC:H surface

even without plasma treatment. In other study, the deposition of TiN from $TiCl_4$ on porous low k such as hydrogen silsesquioxane (HSQ) has produced discontinuous film and chemical analysis has shown that TiN deposition occurred through entire low k materials up to the bottom interface of low k materials, suggesting the need for surface sealing before diffusion barrier deposition.[103,140] To prevent this problem, the surface sealing has been demonstrated by exposure the surface to toluene vapor for porous Si-C-O:H films,.[140]

2. Tantalum and tantalum nitirdes.

Ta is an attractive candidate for Cu interconnect diffusion barrier applications due to its high melting point (2669 °C) and good stability in terms of reaction with Cu.[142-144] The good stability of Ta with Cu is related to the lack of Cu-Ta compound. This is in contrast to Ti, since Cu-Ti compounds are readily formed. There has been significant study of the thermal stability and Cu diffusion barrier properties of Ta thin films. Ta thin films are deposited either as (metastable) tetragonal β phase or cubic α phase depending on growth conditions, substrate materials, and post-deposition annealing.[145,146] While the resistivity of β phase is around 170-210 μΩ cm, that of α phase is much lower, 15-60 μΩ cm.[146,147]

The CVD of Ta films have been studied over several decades.[62] The earliest example of Ta CVD was by direct reduction of Ta halides (without a reactant gas species) which requires a high growth temperature near 2000 °C. This temperature was reduced to 700 to 1200 °C by employing molecular hydrogen as a reducing agent.[148] However, a much lower growth temperature is required for conventional BEOL processes, usually below 400 °C. One of the possible solutions is to use Ta precursors other than halides, such as MO sources. However, similar to Ti case, no good precursor to produce high quality metallic Ta thin films has been

reported.[62,148] The commercially available MO sources, such as $Ta[N(Me)_2]_5$ [pentakis(dimethyamino)tantalum, PDMAT] and TBTDET, contain nitrogen which is incorporated into the film to form nitride. Thus, Ta CVD is impossible from these precursors. Thus, halide precursors are the only commercially available metal precursors for Ta CVD currently. While Ta CVD using chloride requires rather high growth temperature, Ta films were deposited at 450 °C using plasma-enhanced CVD with $TaBr_5$ and hydrogen plasma,[149,150]

The only reported Ta ALD was a plasma enhanced process.[27,43] When $TaCl_5$ was used as metal precursor and atomic hydrogen produced by RF plasma as reducing agent, amorphous Ta thin films have been deposited at temperatures below 250 °C. The as-grown films have resistivity of 150-180 μΩcm and residual Cl contamination between 0.5 - 2 at%. The diffusion barrier properties of PE-ALD Ta films were investigated using test structures shown in Fig. 16a.[27] The ALD Ta barrier films have shown significantly higher failure temperatures compared to PVD Ta; at least 70 °C at comparable thicknesses, which was attributed to the uniform, smooth surface and amorphous or nano-crystalline microstructure of ALD Ta.

TaN also possess high thermal, mechanical, and chemical stability and is used as diffusion barrier for Cu interconnect. Combining these materials, a bilayer structure of Ta/TaN has been used for Cu interconnect diffusion barrier applications, since TaN has good adhesion to silicon oxide and other low k materials and the subsequent PVD Ta is deposited as low resistivity alpha phase.[82] One of the technical difficulties related to the TaN deposition is that TaN has many polymorphs depending on nitrogen content.[151] Among these, the Ta_3N_5 tetragonal phase has very high resistivity, thus less desirable for barrier applications.

The earliest report on ALD of TaN used $TaCl_5$ as metal precursor, which was reacted with NH_3. The deposited film was composed of polycrystalline Ta_3N_5 with very high resistivity,

over 10^4 μΩcm, at above 400 °C.[14,26] This formation of Ta_3N_5, instead of cubic TaN, was attributed to the low reducing power of NH_3. For this particular ALD process, the growth rate and residual film contamination was dependent on the growth temperature. At low growth temperature (200 °C), the growth rate was only 0.12 Å per cycle, while it increased to 0.22-0.24 Å/cycle above 300 °C. Meanwhile, the Cl content was above 20 % at 200 °C, but rapidly decreased to below 0.1 % at above 500 °C. The use of DMHy as an alternative precursor instead of NH_3 also produced high resistivity Ta_3N_5 films.[26] Recent reports on using additional reducing agents such as TMA and amines showed minor improvement in resistivity.[68,69] For TMA, Al incorporation resulted in $TaAl_xN_y$ ternary phase with C contamination.[68] By using Zn as additional reducing agent, cubic TaN with an electrical resistivity as low as 960 μΩcm was obtained, although residual Zn incorporation was problem.[26] TaN ALD using $TaBr_5$, instead of $TaCl_5$, produced similar results.[68,69]

As an alternative approach, the MO Ta source, TBTDET, has been used for ALD and PE-ALD of TaN.[45,46,152] For thermal ALD, NH_3 was used while for PE-ALD atomic H was used as reducing agent. The growth rate for thermal ALD was 1.1 Å/cycle, while that for PE-ALD was 0.8 Å/cycle. XRD has shown that PE-ALD TaN is composed of cubic TaN phase, indicating that the nitrogen in TBTDET is incorporated to TaN film without a contribution from the external nitrogen source. While the resistivity of thermal ALD TaN by MO source was immeasurably high, that of PE-ALD TaN with the same metal precursor was as low as 400 μΩcm. However, the carbon content was quite high (above 15 %) in both films, and the low resistivity of PE-ALD TaN was partially attributed to the formation of TaC, as confirmed by XPS.[46] The formation of TaC, which has considerably lower resistivity (30 μΩcm) than TaN, has been also reported to reduce the resistivity of TaN films at high C content for MO-CVD of TaN.[153] MO-ALD TaN

generally has low film density. The density of thermal MO-ALD TaN was 3.6 g/cm^3, while that of PE-ALD TaN was, though improved, still low as 7.9 g/cm^3 (compared to the bulk value of 16.0 g/cm^3).[46] The step coverage was excellent up to aspect ratio of 10:1. Similarly, TaN using other MO source, $Ta(MeEtN)_5$ [pentakis(methylethylamino)-tantalum, PMEAT], has been recently reported by thermal and PE-ALD and the comparison has shown that deposition rate and density of PE-ALD TaN has higher value.[154]

Recently, low resistivity (350 μΩcm) cubic TaN thin films were grown by PE-ALD using $TaCl_5$ as the metal precursor and a combination of hydrogen and nitrogen in a plasma at low growth temperature of 300 °C.[44] The nitrogen content was easily controlled to produce various TaN phases from Ta to Ta_3N_5 and the N/Ta ratio in the cubic TaN films was controlled from N/Ta = 0.7 up to 1.3 by changing nitrogen partial pressure. The resistivity and growth rate increased with increasing nitrogen concentration in the film. (Fig. 21) The film contained 5-10% oxygen, but subsequent measurements using MEIS have shown that only top 10 Å of TaN films contains O, indicating that this O is incorporated by air exposure.[53]

Diffusion barrier measurement of ALD TaN has been rarely reported. Recent results indicate that the Cu diffusion barrier failure temperature of PE-ALD TaN is comparable to that of PVD TaN.[155] The workfunction of PE-ALD of TaN has been estimated by C-V measurements on SiO_2 as 4.4 eV, which indicates the possible application as n-FET gate metal electrode.[53] ALD TaN grown by TBTDET and NH_3 was reported to show lower leakage current than CVD counterpart on HfO_2-Al_2O_3 laminate high k dielectrics, which was also grown by ALD.[156]

3. Tungsten and tungsten nitrides

As a representative refractory metal, tungsten is hard and inert and has very high melting point with relatively low resistivity (5.6 μΩcm). Tungsten has been one of the most widely used elementary metals in semiconductor devices, especially for contact holes or vias, source, drain, gate metallization, ohmic contact, and diffusion barriers. Since it has very low self diffusivity, tungsten has no concern for electromigration. In addition, stress issue is relatively small since tungsten has low thermal expansion coefficient. Tungsten does not form silicide under 600 °C in contact with Si. Tungsten has three phases: bcc alpha phase with lowest resistivity, metastable beta phase, and fcc gamma phase formed only by sputtering.[62] Tungsten itself and its nitrides form are good diffusion barriers.

W ALD is the most successful case among elemental metal thin films ALD processes reported to date. In addition, various surface analysis techniques have been used for W ALD process and a relatively detailed growth mechanism is known.[25] The primary reason for this is the widespread availability of a good metal precursor, WF_6, and good reducing agent, Si_2H_6 or SiH_4. W CVD using these combinations have been studied and used widely in the semiconductor industry.[62] The overall W CVD process is known to be

$$WF_6(g) + Si_2H_6 \rightarrow W(a) + 2SiHF_3(g)\uparrow + 2H_2(g)\uparrow. \quad (7)$$

As seen in the reaction equation, ideally all Si atoms is removed and only metallic tungsten is deposited.

While the surface reaction by alterative exposure of WF_6 and Si_2H_6 has been studied earlier,[121] the first ALD of W thin film was reported only several years ago.[25] George et al. have used FTIR and spectroscopic ellipsometry to investigate the W ALD process.[25,117] Very smooth tungsten films were deposited at low growth temperatures with growth rates close to ideal 1ML/cycle (2.5 Å/cycle). Neither Si nor F was found in the film, indicating the complete

surface reactions between these two precursors. However, the electrical resistivity was quite high, attributed to the amorphous nature of the grown films. In addition, as mentioned in the previous section, the nucleation of film was difficult on SiO_2 surface.[102] The same authors investigated the nucleation problem of tungsten ALD on SiO_2 using AES as mentioned in the previous section. (Fig. 14) Another reducing agent, B_2H_6 instead of Si_2H_6, has been used with WF_6 for W ALD.[65] Smooth, conformal films with low F content below 0.1% were obtained with resistivity of 150 μΩcm. Additionally, the process using B_2H_6 did not show the nucleation problem for the initial cycles.

Using WF_6 and NH_3, smooth tungsten nitride films were deposited by ALD with the growth rate close to 1 ML/cycle.[117,120] XRD has shown that the films were composed of W_2N polycrystalline grains. The W to N atomic ratio was 3:1, indicating that the control of nitrogen is difficult. Also, the resistivity of the deposited film was very high, about $4.5x10^6$ μΩcm. Similar to W ALD, the nucleation of W_2N ALD was difficult on SiO_2, which was improved by 30 minutes $SiCl_4$ exposure before deposition.[120] At other study using the same precursor set, W_2N film with much lower resistivity (4500 μΩcm) was deposited by ALD with lower deposition rate. [19] The exact reason for the different resistivity is not know, but probably related to the difference in nitrogen content. Also, the latter study has shown that fluoride based W_2N ALD produce much less aggressive pitting on Cu surface compared to chloride based TiN ALD.[19] Recently, PE-ALD of tungsten nitride has been also reported.[157]

WC_xN_y has been deposited from WF_6, NH_3, and $B(Et)_3$ [triethylboron, TEB] for Cu diffusion barrier.[122,140,158] By incorporating TEB, the resistivity decreased considerably, to around 300-400 μΩcm at growth temperature of 300 – 350 °C. The film consisted of nanocrystalline WC_x with low impurity levels (F < 1%, B < 0.5 %). The adhesion of WC_xN_y on

Cu was good without formation of pitting on Cu surface.[158] Also, WC_xN_y was deposited on porous Si-C-O:H films, whose pores were sealed by N_2 plasma treatment.[140] After the pore sealing has been done, WC_xN_y ALD did not show any diffusion of deposited film into the low k materials.

Currently, the commercial W ALD chamber is in the development using similar chemistry. The focus for the current development of W ALD is for nucleation layer deposition for plug fill by CVD W. As one of the modified W ALD processes, pulsed layer nucleation uses WF_6 and SiH_4 with H_2 mixed to produce a higher deposition rate for W nucleation layer deposition.[33] In this case, the continuous flow of H_2 introduced the CVD component (by the reaction of WF_6 and H_2) during deposition and high growth rate as 8-9 Å/cycle was obtained with acceptable conformality.

4. Cu

The precursors for Cu CVD or ALD are classified depending on the electronic status of Cu, which are Cu^I and Cu^{II}. The MO Cu^I precursors include Cu(hfac) and Cu(thd). Currently, the widely studied MO sources for Cu CVD is Cu(hfac)L, where L is a ligand such as trimethoxyvinylsilane (tmvs). For these materials, Cu film deposition by CVD is possible by a disproportionation process,[62]

$$2Cu^IML \rightarrow Cu(s) + Cu^{II}M_2(g)\uparrow + L_2(g)\uparrow. \quad (8)$$

However, this may not be a desirable reaction pathway for ALD since disproportionation disturbs the self-limiting adsorption. Alternatively, a halide source such as CuCl requires a high source temperature above 250 °C to obtain adequate enough vapor pressure for a CVD or ALD process.

For Cu CVD with Cu^{II} precursors, a higher temperature with external reducing agent such as H_2 is required,

$$Cu^{II}M_2' + H_2(g) \rightarrow Cu(s) + 2HM'(g)\uparrow, \quad (9)$$

which is adaptable for an ALD application. Usually, the Cu^{II} source is in the liquid form and readily used as a CVD precursors. The reviews on recent CVD Cu research activity can be found in the literature.[159]

Although the importance of Cu ALD is obvious, only a few reports are available. Usually, the adhesion of the ALD (CVD also) Cu films to the most of dielectrics is bad and usually the deposited films are rough. The first Cu ALD was reported 5 years ago by Ritala et al.[61] CuCl was used as the Cu source and Zn vapor as a reducing agent. Due to the extremely low volatility of CuCl, the vapor was generated by open boat inside the chamber by heating to 390 °C. Although metallic Cu was deposited, self-saturation was not observed. Instead, the growth rate was above 10 Å/cycle, which indicates non-ALD, more CVD-like growth mode. This non-ALD mode growth was attributed to the reversible dissolution of Zn into the deposited Cu film. By the dissolved Zn, the CuCl vapor at the next cycle is reduced resulting in CVD-like deposition.

Later, Cu ALD by CuCl was reported using H_2 as reducing agent.[160-162] On a Ta substrate, the initial reduction of CuCl by Ta produced 300 Å of Cu film by consuming Ta substrate atoms. For deposition on an oxide substrate, no deposition was observed for the same combination of precursors.[61] Due to the disproportionation of CuCl, a slight increase in growth rate was observed for longer CuCl exposure above a semi-saturation condition. Thus, this process is not ideal ALD growth. This process was also a very slow, thermally activated process with the activation energy about 80 kJ/mol.[160] *Ab initio* calculation of CuCl adsorption was

performed and reaction pathways with molecular hydrogen were studied by the same author.[161,162] By comparison of molecular hydrogen adsorption activation energy, the rate limiting step was suggested to be the reaction between adsorbed CuCl and molecular hydrogen rather than the dissociative adsorption of hydrogen on Cu surface.

More recently, Cu ALD using MO sources have been studied by several authors. Cu ALD on various surface was studied using $Cu(thd)_2$ + H_2.[59,163] The deposited films contained low O and C content, but with a factor of five higher resistivity than bulk value. The ALD process window was found to be between 190 – 260 °C and the selectivity between Pt-seeded and unseeded area was observed at this temperature region. Above this temperature, the selectivity was broken with growth rate increase due to the thermal decomposition of the precursors. While ALD of Cu using these precursors was observed on various pure metal substrates, deposition was not successful on some oxides. This observation was explained by uncompleted dissociation of $Cu(thd)_2$ adsorption on hydroxyl group. More recently, a common CVD precursor, $Cu(hfac)_2 \cdot xH_2O$, was used for ALD of Cu by Solanki et al.[60] Three different reducing agents, methanol (CH_3OH), ethanol (C_2H_5OH), and formalin (HCHCO), were used. Among these three reducing agents, the formalin produced best results. The resistivity of the grown polycrystalline Cu film was 1.78 μΩcm for 120 nm thick film. For 20 nm thick film, higher resistivity was obtained, attributed to the thickness effect of resistivity. In other reports, ALD Cu films were deposited on Ti, Al, and glass surfaces using $Cu(acac)_2$ [Cu^{II}(acetylacetonate)$_2$; acac = $CH_3COCHCOCH_3$] and H_2.[51] But due to thermal decomposition of the precursor, true ALD process was not realized at the investigated temperature of 250 °C. More recently, the Cu deposition by reduction of ALD CuO was reported.[164] In this process, the CuO was deposited by the reaction between $Cu(thd)_2$ and O_3 and the deposited CuO was reduced

by ethanol. By this way, Cu film with resistivity of 10 μΩcm with carbon content below 0.1 % was obtained.

5. Ternary nitrides

Since grain boundaries play such an important role as diffusion pathways for Cu, the ternary phase of materials such as $TiSi_xN_y$, $TaSi_xN_y$, WSi_xN_y, WC_xN_y, or WB_xN_y have been expected to be a good diffusion barrier.[86,140,165,166] While the usual binary nitrides crystallize easily by annealing even when they were amorphous in their as-deposited condition, the ternary phase remains amorphous up to a much higher temperature. In addition, $TaSi_xN_y$ and $TiAl_xN_y$ are being currently investigated as metal gate electrodes due to their high thermal stability and proper electrical performances.[167,168] Additionally, $TiAl_xN_y$ has high oxidation resistance at elevated temperatures.[169]

Even with this technical importance, only a few reported works exist on ALD of ternary nitrides. For ternary nitrides ALD, an additional source for Si or Al is added to the existing binary ALD precursor set. Kang et al. reported the $TiSi_xN_y$ ALD using TDMAT, with NH_3 and SiH_4 precursors at a temperature of 180 °C, focusing on the effects of Si incorporation.[55,108,170] Compared to TiN ALD using TDMAT and NH_3, the growth rate for $TiSi_xN_y$ decreased from 4.4 Å/cycle to 2.2 Å/cycle with increasing SiH_4 pressure when TDMAT–NH_3–SiH_4 pulses are introduced consequently. This was interpreted as the SiH_4 adsorption produces blockade toward the adsorption of TDMAT, since no reaction was found between SiH_4 and either TDMAT or NH_3. The Si content in the film remained constant at 18 % after saturation, while during CVD using same precursors the Si content increases logarithmically with SiH_4 partial pressure.[171] When SiH_4 and NH_3 were supplied at the same time, the growth rate sharply decreased by more

than an order of magnitude with SiH_4/NH_3 flow ratio increase.[108] By changing the combination of the number of TiN ALD and $TiSi_xN_y$ ALD sequences, systematic control of the Si content and growth rate was demonstrated.[55] TEM analysis has shown the films are mainly amorphous with some nano crystalline TiN grains.[55] Good conformality was obtained on the structures with aspect ratio of 10:1. However, the resistivity was very high, above 30,000 μΩcm. Diffusion barrier properties, estimated by Cu MOS capacitor structure and C-V characterizations, showed the $TiSi_xN_y$ ALD film with 10 nm thickness to be an excellent barrier up to 800 °C for 60 min annealing.[108]

More recently, $TiSi_xN_y$ PE-ALD using $TiCl_4$, SiH_4, and nitrogen/hydrogen plasma has been reported.[134] Depending on the precursor exposure sequence, $TiSi_xN_y$ films with 500 – 1000 μΩcm resistivity were obtained at 350 °C. The Si content, resistivity, and growth rate were lower when a $TiCl_4$-SiH_4-plasma sequence was used, compared to SiH_4-$TiCl_4$-plasma sequence. XPS results indicated that Si is present as a form of Si_3N_4 in the films, which resulted in resistivity increase with Si content. Diffusion barrier properties, investigated by resistivity and XRD, indicated that the barrier failure temperature became higher with Si incorporation.

Similarly, $TaSi_xN_y$ PE-ALD has been performed using $TaCl_5$, SiH_4, and nitrogen/hydrogen plasma.[53] Similar to the $TiSi_xN_y$ PE-ALD case, the precursor exposure sequence affected the growth rate and film properties. With $TaCl_5$-SiH_4-plasma sequence, amorphous films with lower resistivity (below 1000 μΩcm) were deposited, while high resistivity (above 10^5 μΩcm), polycrystalline TaN was deposited for the SiH_4-$TaCl_5$-plasma sequence.

Both inorganic and MO source have been used for $TiAl_xN_y$ ALD. From $TiCl_4$, DMAH-EPP, and NH_3 precursors, ALD $TiAl_xN_y$ was performed at 400 °C.[72] Films with low Cl content

(< 0.5 at. %) were grown with an Al concentration below 10 %. The deposited films were polycrystalline and the growth rate was much higher than that of TiN ALD. The resistivity was 400 μΩcm, which is low for ternary nitrides. Similarly, MO-ALD of $TiAl_xN_y$ using TDMAT as the Ti precursor was investigated at a growth temperature of 200 ºC.[73,74] However, the C content was as high as 25 % and the resistivity was over 1500 μΩcm. Additionally, as mentioned in the previous sections, using TMA as an additional reducing agent for either TiN and TaN ALD always resulted in a significant Al impurity level, producing in Ti(or Ta)Al_xN_y film deposition.

The microstructure of ALD $TiAl_xN_y$ film was amorphous up to 900 ºC annealing. The Cu diffusion barrier properties of $TiAl_xN_y$ films were also studied for both precursor sets. The comparison study between ALD TiN and ALD $TiAl_xN_y$ using MO source has shown that the ALD $TiAl_xN_y$ films have over 200 ºC higher Cu diffusion barrier failure temperature, as measured from XRD and etch-pit test.[74] However, another study has shown that the diffusion barrier properties of ALD $TiAl_xN_y$ tested by XRD, Secco etch analysis, and resistivity measurements did not show superior result compared to ALD TiN, which fails at 500 to 600 °C for a 10 nm thick film.[52]

6. Other metals/nitrides

6.1. NbN, Mo/MoN_x

NbN has tribological applications due to its desirable mechanical properties and also has potential application as a superconductor with a relatively high critical temperature (T_c = 15 K). ALD of NbN has been performed using $NbCl_5$ and NH_3, reported more than 15 years ago.[14] The growth temperature was 500 ºC and a polycrystalline film with resistivity of 240 μΩcm was

deposited. The growth rate was 0.25 Å/cycle, close to thoseof other ALD transition metal nitrides. The T_c for superconductivity was measured as about 9.5 K. The addition of Zn to the same precursor combination produced lower resistivity films.[172] However, long exposure of $NbCl_5$ resulted in growth rates decrease, indicating the etching of NbN by $NbCl_5$. In addition, the grain size of ALD NbN films increased by addition of Zn.[126] However, a growth temperature below 400 ºC produced high resistivity films (>10^4 μΩcm) with high Cl content (>15 %). DMHy was used instead of NH_3 as an attempt to lower the growth temperature, producing minor improvement.[67]

Mo is a good electrode materials for thin film electroluminescence devices and also has potential application as metal gate electrode for CMOS.[64] The ALD of metallic Mo film was done using $MoCl_5$ and Zn as precursors.[64] At a growth temperature of 400-500 ºC, polycrystalline films with resistivity of 15 μΩcm were deposited. However, similar to Cu ALD, a CVD-like process was observed due to the dissolution of Zn to Mo. In addition, etching of Mo by $MoCl_5$ was found to destroy the ALD process. Thus, the real ALD mode growth could not be achieved. MoN_x ALD using $MoCl_5$ and NH_3 at 500 ºC produced a polycrystalline mixture of cubic MoN_2 and hexagonal MoN.[14] At 400 ºC, however, the resistivity of the MoN_x film was immeasurably high with about 10 % Cl content.[67] Later attempts to lower the deposition temperature by the use of Zn as an additional reducing source or DMHy as alternative for NH_3 resulted in marginal improvement in the film properties at 400 ºC. In all cases, the resistivity was quite high (above 900 μΩcm). Moreover, the use of DMHy incorporated about 10 % C in the film.

6.2. Ni, Ru, Pt, Al

Although elemental Ni thin film is not an important material for current semiconductor device fabrication, Ni monosilicide is being studied intensively to replace Co disilicide, especially for contact layers of high speed, strained Si CMOS devices.[173] Ni ALD has been reported using $Ni(acac)_2$ as a metal precursor.[51] At 250 ºC of growth temperature, two different methods were attempted. The first method was a conventional ALD using H_2 as the reduction agent, producing H(acac) as by-product. While Ni was deposited on Ti and Al substrates by this way, little growth was found on Si and SiO_2. Alternatively, the same metal precursor was reacted with H_2O or O_3 in an ALD mode to produce Ni-oxide layer, which was then reduced to a metal layer by exposure to molecular hydrogen at elevated temperature. The growth rate of the latter process was 0.3-0.5 Å/cycle (for NiO), and NiO was deposited even on SiO_2. Reduction to Ni was done in a furnace at 230 ºC with 5% He in Ar environment. Recently, another technique for reduction of NiO was introduced.[66] In this approach, NiO was deposited using $Ni(Cp)_2$ and H_2O, and after each cycle, a hydrogen plasma was introduced to reduce the deposited oxide. By this technique, metallic Ni was obtained, although the C content was above 5%.

Ru has several good properties such as good etching property and high thermal and chemical stability.[174,175] Recently, Ru is receiving extensive attention due to its good properties as electrode in DRAM applications,[93] a metal gate electrode for CMOS,[176] and a potential seed layer for direct plating of Cu electrodeposition in interconnect applications[89]. A simple way of depositing metallic Ru by ALD has been reported recently.[49,50,101] $Ru(Cp)_2$ or $Ru(Od)_3$ [Od = 2,4-octanedionate] was used as metal precursors which reacted with O_2 to produce Ru thin films in an ALD mode. The ALD process was attributed to the oxidative decomposition of Ru precursor ligands by oxygen molecules, producing CO_2 and H_2O as byproducts. Polycrystalline Ru films with low resistivity (17-18 μΩcm) were deposited on *in-situ* grown ALD Al_2O_3 and

TiO_2 layer.[50] On SiO_2 surface, however, the deposited films were non-uniform with macroscopic defects. This was attributed to the difference in the surface density of hydroxyl group, which promote uniform nucleation of Ru films on oxide surface. The reported impurity levels in the films were quite low (H, C, O < 1%).[49] RuO_2 was not deposited with the studied experimental conditions.

Pt has potentially similar applications as Ru in semiconductor devices. Two different techniques for ALD of Pt have been reported so far. The first is the deposition of Pt oxide by ALD using $Pt(acac)_2$ with an oxidant such as H_2O and O_3, which is then reduced to metallic Pt by hydrogen exposure, similar to Ni.[51] A second technique is the direct deposition of Pt using $Me(Et)Pt(Me)_3$ as metal precursor with oxygen, similar to Ru ALD.[49]

Although Al has been primary interconnect materials and one of the most widely used metals for semiconductor devices, there has been little report on Al ALD yet. Recently, Al PE-ALD was reported using TMA and atomic H as precursors.[177] Rather high resistivity film (10 μΩcm) with 3-4 % of C and H contaminant was deposited at 250 ºC. The deposited film has good step coverage with smooth surface.

VI. Problems to be solved and future challenges.

Recently, the interest in ALD of metals and nitrides in semiconductor process has become intensive.[178] However, ALD of metals and nitrides are still in the early development stage with many technical issues to be resolved. Some of the key issues include; 1) development of good precursors with adequate properties, 2) studies of surface reaction chemistry, 3) deposition of ALD metals/nitrides on various surfaces including Cu and low k materials, 4) development of good analytical techniques, ideally *in-situ*, for films which are often only a few

nm in thickness, 5) detailed studies of film properties and their effects on device applications, and 6) comparisons of the ALD film properties with those of other deposition techniques.

The success of ALD process starts with good selection of precursors. Compared to the more widely investigated ALD of oxides, rather limited precursors exist for ALD of metals and nitrides. Until recently, most of the precursors that have been used for ALD in the metals and nitrides families have been directly adapted based upon previous works for CVD. Although ALD has many similarities to CVD, the requirements for good ALD precursors are clearly different from their CVD parallels. For example, while the volatility (and vapor pressure) is very important for a CVD process, which requires continuous flows, it is less critical for ALD which operates in a pulsed manner with low net flow. In fact, other properties of the precursor, such as self-adsorption, nucleation and reaction with surface are more important in the ALD mode compared to CVD. This suggests that in addition to the existing CVD precursors, new precursors applicable to ALD alone need to be developed with parallel efforts of estimating already existing CVD precursors for ALD process.

As mentioned above, the ALD proceeds through surface reactions. However, too little information exists on the surface chemistry and reaction of the precursors with substrate materials. It is needles to say that molecular level surface science study would be essential. By these studies, important growth mechanism related issues could be addressed. The understanding of the reaction of precursors with various surfaces is still premature, thus there are only a few reports even for the most widely employed $TiCl_4$ precursor. In addition, while the initial surface condition including various surface treatments and interaction of precursors with various surfaces is important, the systematic study on these subjects has been rare. As an example, the use of hydrogen as a reducing agent for many ALD processes can result in etching of the

substrate. This is of particular concern to the case of low-k, polymeric dielectrics, which are etched spontaneously in atomic hydrogen. As pointed out in the previous report, the compatibility of ALD process with certain low k materials are one of the biggest issue for BEOL process.[103] Also, the need for use of porous low k materials for dielectric constant below 2 would add additional difficulty in deposition of continuous diffusion barrier materials by ALD. For all these surface science related problems, more easy to use, powerful surface analysis technique will give valuable information.

Related to the surface reaction study, other characteristics of ALD need to be further studied. One of them is selective growth of metal/nitride film by ALD. The selective growth of CVD has not been so successful, but ALD has better chance since the ALD occurs by surface reactions. Additionally, the nucleation of ALD process on various surfaces is a practically important matter. The nucleation of ALD films is entirely dependent upon substrate materials and the modern semiconductor fabrication introduces novel materials continuously, including low k and various metal/nitride/oxides/silicides. Moreover, as the diffusion barrier thickness gets even smaller, the nucleation process should be considered precisely, since the portion of initial cycles among the total number of cycles becomes larger for very thin films.

In addition to these scientific studies, questions remain regarding the properties of the metal and nitride ALD films and their effects on semiconductor device properties. For the implementation of ALD films to device fabrication, there are many performance-related problems to be investigated, such as conformality and reliability properties including electromigration resistance and time-dependant electrical properties. One of the concerns of ALD thin films is the common contaminant such as Cl, C, or H. More systematic and detailed study should be performed how these can affect the device performance. One of the useful

approachs would be the comparative study of ALD metal and nitride films with those deposited by other techniques. The pros and cons of replacing currently used deposition techniques with ALD should be carefully examined.

VII. Summary

In this paper, the various aspects of metal and nitride ALD thin films focusing on their applications in modern semiconductor device fabrication have been reviewed. ALD is a very promising thin film deposition technique for metal/nitrides used in semiconductor device fabrication, due to its ability in producing thin films with excellent conformality with atomic scale control. The ALD of metals and nitrides are in early stage of the development, yet the implementation of this thin film technique is imminent issue. The implementation of ALD technique to real device process would require more deep understanding on the process as well as the deposited film properties.

Acknowledgments

The author gratefully acknowledges Dr. Steve Rossnagel and Dr. Dan Edelstein at IBM research and Prof. Hyeongtag Jeon for their fruitful discussions and insightful comments. I also thank Dr. Mikko Ritala, Prof. Steve M. George, Dr. Michel Chudzick, Dr. Yo-Sep Min, and Prof. Joseph E Greene for their kindness, giving me permission to use their figures in this paper.

References

1. T. Suntola, Mater. Sci. Rep. **4**, 265 (1989).

2. T. Suntola, Thin Solid Films, **216**, 84 (1992).

3. C.H. Goodman and M.V. Pessa, J. Appl. Phys. **60**, R65 (1986).

4. S.M. Bedair, J. Vac. Sci. Technol. **B12**, 179 (1994).

5. M. Leskelä and M. Ritala, Journal de Physique. IV, **9**, Pr8-837 (1999).

6. *The International Technology Roadmap for Semiconductors*, 2001 edition.

7. "Handbook of Semiconductor Manufacturing Technology", ed by Y. Nishi and R. Doering, Marcel Dekker, Inc. 2000.

8. S.M. Rossnagel, J. Vac. Sci. technol. **B16**, 2585 (1998).

9. S.M. Rossnagel and H. Kim, Proc. of the IEEE 2001 International Interconnect Technology Conference 3, (2001).

10. M. Ritala and M. Leskelä, in H.S. Nalwa (Ed.), *Handbook of Thin Film Materials*, vol. 1, Academic Press, San Diego, CA, 2001, p. 103.

11. M. Ritala, Appl. Surf. Sci. **112**, 223 (1997).

12. M. Ritala and M. Leskelä, Nanotechnology **10**, 19 (1999).

13. M. Leskelä and M. Ritala, Thin Solid Films **409**, 138 (2002).

14. L. Hiltunen, M. M. Leskelä, M. Makelä, L. Ninistö, E. Nykänen, and P. Soinen, Thin Solid Films, **166**, 154 (1988).

15. H. Jeon, J.-H. Koo, J.-W. Lee, Y.-S. Kim, K. M. Kang, Y. D. Kim, and Y. D. Kim, Mat. Res. Soc. Symp. Proc. **616**, 211 (2000).

16. M. Ritala, M. Leskelä, E. Rauhala, and P. Haussalo, J. Electrochem. Soc. **142**, 2731 (1995).

17. A. Satta, G. Beyer, K. Maex, K. Elers, S. Haukka, and A. Vantomme, Mat. Res. Symp. Proc. **612**, D6.5.1 (2000).

18. C.H. Ahn, S.G. Cho, H.J. Lee, K.H. Park, and S.H. Jeong, Metals and materials International **7**, 621 (2001).

19. K.-E. Elers, V. Saanila, P. J. Soininen, W.-M. Li, J.T. Kostamo, S. Haukka, J. Juhanoja, and W.F. A. Besling, Chem. Vap. Deposition, **8**, 149 (2002).

20. W. Chen and J.T. Roberts, Surface Science **359**, 93 (1996).

21. T. Mitsui, E. Hill, R. Curtis, and E. Ganz, J. Vac. Sci. Technol. **A19**, 563 (2001).

22. H. Kim and S.M. Rossnagel, J. Vac. Sci. Technol. **A20**, 802 (2002).

23. M. Juppo, A. Rahtu, and M. Ritala, Chem. Mater. **14**, 281 (2002).

24. T. R. Bramblett, Q. Lu, T. Karasawa, M.-A. Hasan, S. K. Jo, and J. E. Greene, J. Appl. Phys. **76**, 1884 (1994).

25. J.W. Klaus, S.J. Ferro, and S.M. George, Thin Solid Films **360**, 145 (2000).

26. M. Ritala, P. Kalsi, D. Riihelä, K. Kukli, M. Leskelä, and J. Jokinen, Chem. Mater. **11**, 1712 (1999).

27. H. Kim, C. Cabral, Jr., C. Lavoie, and S.M. Rossnagel, J. Vac. Sci. Technol. **B20**, 1321 (2002).

28. K. Kukli, M. Ritala, and M. Leskelä, J. Appl. Phys. **86**, 5656 (1999).

29. Z. Wang and S. Oda, J. Electrochem. Soc. **147**, 4615 (2000).

30. J.Y. Kim, H.K. Kim, S.W. Seo, Y. Kim, Y.D. Kim, and H. Jeon, American Vacuum Society Topical Conference on Atomic Layer Deposition 2001, Monterey (2001).

31. Z. Sechrist, F.H. Fabreguette, O. Heintz, and S.M. George, American Vacuum Society Topical Conference on Atomic Layer Deposition 2002, Seoul (2002).

32. A.P. Paranjpe, B. McDougall, K.Z. Zhang, W. Vereb, American Vacuum Society Topical Conference on Atomic Layer Deposition 2002, Seoul (2002).

33. S.-H. Lee, P. Wongsenakhum, L. Gonzale, J. Gao, L. Chan, J. Collins, K. Ashtiani, and K. Levy, American Vacuum Society Topical Conference on Atomic Layer Deposition 2002, Seoul (2002).

34. Z. Zhang, C.A. Bercaw, T.D. Nguyen, and T. Nguyen, American Vacuum Society Topical Conference on Atomic Layer Deposition 2002, Seoul (2002).

35. K. Jun, Y.-H. Shin, and Y. Shimogaki, American Vacuum Society Topical Conference on Atomic Layer Deposition 2002, Seoul (2002).

36. K.-E. Elers, V. Saanila, P.J. Soininen, S. Hauuka, Advanced Metallization Conference 2000 (AMC 2000), Proceedings of the Conference 295 (2000).

37. J. Nishizawa, A, Murai, T. Oizumi, T. Kurabayashi, K. Kanamoto, and T. Yoshida, J. Cryst. Growth **233**, 161 (2001).

38. D. Lubben, R. Tsu, T.R. Bramblett, and J.E. Greene, J. Vac. Sci. Technol. **A9**, 3003 (1991).

39. F. Greer, J.W. Coburn, D. Fraser, and D.B. Graves, American Vacuum Society Topical Conference on Atomic Layer Deposition 2001, Monterey (2001).

40. F. Greer, D. Fraser, J.W. Coburn, and D.B. Graves, J. Vac. Sci. Technol. **A21**, 96 (2003).

41. *Handbook of plasma processing technology: Fundamentals, Etching, Deposition, and surface interactions*, Ed. S.M. Rossnagel, J.J. Cuomo, and W.D. Westwood, Noyes publications, NJ.

42. R. Reif and W. Kern, "Plasma-Enhanced Chemical Vapor Deposition," in *Thin Film Process II*, edited by J.L. Vossen and W. Kern, Academic Press, 1991.

43. S.M. Rossnagel, A. Sherman, and F. Turner, J. Vac. Sci. Technol. **B18**, 2016 (2000).

44. H. Kim, A.J. Kellock, and S.M. Rossnagel, J. Appl. Phys. **92**, 7080 (2002).

45. J.-S. Park, M.J. Lee, C.-S. Lee, and S.-W. Kang, Electrochem. Sold State Lett. **4**, PC17 (2001).

46. J.-S. Park, H.-S. Park, and S.-W. Kang, J. Electrochem. Soc. **149**, C28 (2002).

47. J.M. Jasinski, Chem. Phys. Lett. **211**, 564 (1993).

48. M.N. Rocklein and S.M. George, American Vacuum Society Topical Conference on Atomic Layer Deposition 2002, Seoul (2002).

49, T. Aaltonen, M Ritala, and M. Leskelä, American Vacuum Society Topical Conference on Atomic Layer Deposition 2002, Seoul (2002).

50. T. Aaltonen, P. Alén, M Ritala, and M. Leskelä, Chemical Vapor Deposition, in press.

51. M. Utriainen, M. Krönger-Laukkanen, L.-S. Johansson, and L. Niinistö, Appl. Surf. Sci. **157**, 151 (2000).

52. M. Juppo, P. Alen, M. Ritala, and M. Leskelä, Chem. Vap. Deposition **7**, 211 (2001).

53. H. Kim and S.M. Rossnagel, 49th International American Vacuum Society Conference, Denver (2002).

54. J-S. Min, Y.-W. Son, W-G. Kang, S.-S. Chun, and S.-W. Kang, Jpn. J. Appl. Phys. **37**, 4999 (1998).

55. J-S. Min, J.-S. Park, H.-S. Park, and S.-W. Kang, J. Electrochem. Soc. **147**, 3868 (2000).

56. J.-W. Lim, J.-S. Park, and S.-W. Kang, J. Appl. Phys. **87**, 4632 (2000).

57. J.-H. Yun, E.-S. Choi, C.-M. Jang, and C,-S. Lee, Jpn. J. Appl. Phys. Pt2. **41**, L418 (2002).

58. D.-J. Kim, Y.-B. Jung, M.-B. Lee, Y.-H. Lee, J.-H. Lee, and J.-H. Lee, Thin Solid Films **372**, 276 (2000).

59. P. Mårtensson and J.-O. Carlsson, J. Electrochem. Soc. **145**, 2926 (1998).

60. R. Solanki and B. Pathangey, Electrochem. Solid-State Lett. **3**, 479 (2000).

61. M. Juppo, M. Ritala, and M. Leskelä, J. Vac. Sci. Technol. **A15**, 2330 (1997).

62. T. Kodas and M. Hampden-Smith, *The chemistry of metal CVD*, VCH Publishers Inc., New York, 1994.

63. R.K. Grubbs and S.M. George, 49th International American Vacuum Society Conference, Denver (2002).

64. M. Juppo, M. Vehkamäki, M. Ritala, and M. Leskelä, J. Vac. Sci. Technol. **A16**, 2845 (1998).

65. M. Yang, H. Chung, A. Yun, H. Fang, A. Zhang, C. Knepfler, R. Jackson, J.S. Byun, A. Mak, M. Eizenberg, X. Moshi, M. Xi, M. Kori, and A.K. Sinha, Advanced Metallization Conference 2001 (AMC 2001) 655 (2001)

66. H. Chae, H.-S. Park, and S.-W. Kang, Electrochem. Solid-State Lett. **5**, C64 (2002).

67. M. Juppo, M. Ritala, and M. Leskelä, J. Electrochem. Soc. **147**, 3337 (2000).

68. P, Alén, M. Juppo, M. Ritala, T. Sajavaara, J. Keinonen, and M. Leskelä, J. Electrochem. Soc. **148**, G566 (2001).

69. Alen1. P, Alén, M. Juppo, M. Ritala, M. Leskelä, T. Sajavaara, and J. Keinonen, J. Mater. Res. **17**, 107 (2002).

70. S. Seo, J. Kim, Y. Kim, Y.D. Kim, H. Jeon, 49th International American Vacuum Society Conference, Denver (2002).

71. D.-G. Park, K-Y. Lim, H.-J. Cho, T.-H. Cha, I.-S. Yeo, J.-S. Roh, and J.W. Park, Appl. Phys. Lett. **80**, 2514 (2002).

72. J. Koo, J.-W. Lee, T. Doh, Y. Kim, Y.-D. Kim, and H. Jeon, J. Vac. Sci. Technol. **A19**, 2831 (2001).

73. J.Y. Kim, H.K. Kim, Y. Kim, Y.D. Kim, and H. Jeon, Jpn. J. Appl. Phys. Pt. 1 **41**, 562 (2002).

74. J.Y. Kim, H.K. Kim, Y. Kim, Y.D. Kim, W.M. Kim, and H. J. Korean Soc. **40**, 176 (2002).

75. S. P. Murarka, Materials Science and Engineering **R19**, 87 (1997).

76. Y. Shacham-Diamand, J. Electronic materials **30**, 336 (2001).

77. S. Hauka, K.E. Elers, and M. Tuominen, Mat. Res. Soc. Symp. Proc. **612**, 1 (2001).

78. C.-K. Hu, R. Rosenberg, H.S. Rathore, D.B. Nguyen, and B. Agarwala, Proc. of the IEEE 1999 International Interconnect Technology Conference 267 (1999).

79. S.P. Murarka, R.J. Gutmann, A.E. Kaloyeros, W.A. Lanford, Thin Solid Films **236**, 257 (1993).

80. M.A. Nicolet, Thin Solid Films, **52**, 415 (1978).

81. J. Torres, Appl. Surf. Sci. **91**, 112 (1995).

82. D. Edelstein, C. Uzoh, C. Cabral, Jr., P. DeHaven, P. Buchwalter, A. Simon, E. Cooney, S. Malholtra, D. Klaus, H. Rathore, B. Ararwala, and D. Nguyen, Proc. of the IEEE 2001 International Interconnect Technology Conference, 9 (2001).

83. D. Edelstein, J. Heidrenreich, R. Goldblatt, W. Cotte, C. Uzoh, N. Lustig, P. Roper, T. McDevitt, W. Mostiff, A. Simon, J. Dukovic, R. Wachnik, H. Rathore, R. Schulz, L. Su, S. Luce, and J. Slattery, Tech. Digest. 1997 IEEE International Electron Device Meeting, 773 (1997).

84. H.P. Kattelus, M.-A. Nicolet, in D. Gupta, P.S. Ho (eds.) *Diffusion phenomena in thin film and microelectronic materials*, Noyes Publications, Park Ridge, NY, (1989).

85. C.K. Hu, S. Chang, M.B. Small, and J.E. Lewis, Proc. IEEE VLSI Multilevel Interconnect Conf. 181 (1986).

86. M.-A. Nicolet, Appl. Suf. Sci. **91**, 269 (1995).

87. P. Andricacos, IBM J. Res. Development **42**, 567 (1998).

88. R. Rosenberg, D.C. Edelstein, C.-K. Hu, and K.P. Rodbell, Annual Review of Materials Science **30**, 229 (2000).

89. M.W. Lane, C.E. Murray, F.R. McFeely, P.M. Vereecken, and R. Rosenbaum, Proc. of the IEEE 2003 International Interconnect Technology Conference, in press.

90. H.-S. P. Wong, IBM J. Res. Dev. **46**, 133 (2002).

91. D.-G. Park, K-Y. Lim, H.-J. Cho, T.-H. Cha, J.-J. Kim, J.-K. Ko, I.-S. Yeo, and J.W. Park, 2001 Symposium on VLSI Technology. Digest of Technical Papers 65 (2001).

92. A. Chaterjee, R.A. Chapman, G. Dixit, J. Kuehne, S. Hattangady, H. Yang, G.A. Brown, R. Aggarwal, U. Erdogan, Q. He, M. Hanratty, D. Rogers, S. Murtaza, S.J. Fang, R. Kraft, A.L.P. Rotondaro, J.C. Hu, M.; Terry, W. Lee, C. Fernando, A. Konecni, G. Wells, D. Frystak, C. Bowen, M. Rodder, and I.-C. Chen, IEDM Tech. Digest 821 (1997).

93. B.K. Moon, J. Aoyama, and K. Kator, Appl. Phys. Lett. 74, 824 (1999).

94. L.K. Elbaum and M.W. Wittmer, J. Electrochem. Soc. 135, 2610 (1988).

95. J.W. Kim, S.D. Nam, S.H. Lee, S.J. Won, W.D. Kim, C.Y. Yoo, Y.W. Park, S.I. Lee, M.Y. Lee, Jpn. J. Appl. Phys. Pt. 1. **39**, 2094 (2000).

96. T. Aoyama and K. Eguchi, Jpn. J. Appl. Phys. **38**, L1134, (1999).

97. Y. Matsui, M. Hiratani, T. Nabatame, Y. Shimamoto, and S. Kimura, Electrochem. Solid-State Lett. **5**, C18, (2002).

98. J.-H. Lee, J.-Y. Kim, S.W. Rhee, D.Y. Yang, D.-H. Kim, C.-H. Yang, Y.-K. Han, and C.-J. Hwang, J. Vac. Sci. Technol. **A18**, 2400 (2000)

99. J. Lutzen, A. Birner, M. Goldbach, M. Gutsche, T. Hecht, S. Jakschik, A. Orth, A. Sanger, U. Schroder, H. Seidl, B. Sell, D. Schumann, 2002 Symposium on VLSI Technology. Digest of Technical Papers 178 (2002)

100. M. Chudzik, N. Edleman, P. Shafer, D. Park, A. Chakravarti, R. Divakaruni and R. Jammy, Proc. 2003 Electrochemical Society Meeting, in press.

101. Y.-S. Min, E. J. Bae, K.S .Jeong, Y.J. Cho, J.-H. Lee, and W.B. Choi, American Vacuum Society Topical Conference on Atomic Layer Deposition 2002, Seoul (2002).

102. J.W. Elam, C.E.Nelson, R.K. Grubbs, and S.M. George, Thin Solid Films **386**, 41 (2001)

103. G. Beyer, A. Satta, Jörg Schuhmacher, K. Maex, W. Besling, O. Kilpela, H. Sprey, and G. Tempel, Microelectronic Engineering **64**, 233 (2002).

104. Roy G. Gordon, Jill Becker, Dennis Hausmann, and Esther Kim, American Vacuum Society Topical Conference on Atomic Layer Deposition 2002, Seoul (2002).

105. S. Smith, W.-M. Li, K.-E. Elers, and K. Pfeifer, Microelectronic Engineering **64**, 247 (2002).

106. *Semiconductor material and device characterization*, D.K. Schroder, John Wiley and Sons, Inc. New York 1998.

107. J. Uhm and H. Jeon, Jpn. J. Appl. Phys. **40**, 4657 (2001).

108. J-S. Min, H.-S. Park, and S.-W. Kang, Appl. Phys. Lett. **75**, 1641 (1999).

109. M.W. Lane, R.H. Dauskardt, N. Krishna, and I. Hashim, J. Mater. Res. **15**, 203 (2000).

110. H. Kim, unpublished.

111. C. H. Peng, C. H. Hsieh, C. L. Huang, J. C. Lin, M. H. Tsai, M. W. Lin, C. L. Chang, Winston S. Shue, and M. S. Liang, IEDM Tech. Digest 2002

112. J.W. Elam, M.D. Groner, and S.M. George, Rev. Sci. Instruments **73**, 2981 (2002).

113. A. Rahtu and M. Ritala, Appl. Phys. Lett. **80**, 54 (2002).

114. A. Rahtu, T. Alaranta, and M. Ritala, Langmuir, **17**, 6506 (2001).

115. R. Matero, A. Rahtu, and M. Ritala, Chem. Mater. **13**, 4506 (2001).

116. J. Aarik, K. Kukli, A. Aidla, and L. Pung, Appl. Surf. Sci. **103**, 331 (1996).

117. J.W. Klaus, S.J. Ferro, and S.M. George, Appl. Surf. Sci. **162-163**, 479 (2000).

118. A. Rahtu and M. Ritala, Chem. Vap. Deposition **13**, 817 (2001).

119. M. Ritala, M. Juppo, K. Kukli, A. Rahtu, and M. Leskelä, J. Phys. IV, Proc. (France) **9**, 1021 (1999).

120. J.W. Klaus, S.J. Ferro, and S.M. George, J. Electrochem. Soc. **147**, 1175 (2001).

121. Y. Yamamoto, T. Matsuura, and J. Murota, Surface Science **408**, 190 (1998).

122. W.-M. Li, K. Elerrs, J. Kostamo, S. Kaipio, H. Huotari, M. Soininen, P.J. Soininen, M. Tuominen, S. Kaukka, S. Smith, and W. Besling, Proc. of the IEEE 2002 International Interconnect Technology Conference 191 (2002).

123. M. Schuisky, J.W. Elam, and S.M. George, Appl. Phys. Lett. **81**, 180 (2002).

124. S. Riede, S.E. Schulz, and T. Gessner, Microelectronic Engineering **50**, 533 (2000).

125. M. Ritala, M. Leskelä, J.-P. Dekker, C. Mutsaers, P. J. Soinen, and J. Skarp, Chemical Vapor Deposition **5**, 7 (1999).

126. M. Ritala, T. Asikainen, M. Leskelä, J. Jokinen, R. Lappalainen, M. Utriainen, L. Niinist, and E. Ristolainen, Appl. Surf. Sci. **120**, 199 (1997).

127. M. Juppo, P. Alen, M. Ritala, T. Sajavaara, J. Keinonen, and M. Leskelä, Electrochemical and Solid-State Letters, **5**, C4 (2002).

128. H. Jeon, J.-W. Lee, YD. Kim, D.S. Kim, and K.-S. Yi, J. Vac. Sci. Technol. **A18**, 1595 (2000).

129. M. Ritala, M. Leskelä, E. Rouhala,and J. Jokinen, J. electrochem. Soc. **145**, 2914 (1998).

130. C. Faltermeier, C. Goldberg, M. Jones, A. Upham, D. Manger, G. Peterson, J. Lau, A.E. Kaloyeros, B. Arkles, and A. Paranjpe, J. Electrochem. Soc. **144**, 1002 (1997).

131. J.-W. Lim, J.-S. Park, and S.-W. Kang, J. Electrochem. Soc. **148**, C403 (2000).

132. J.-W. Lim, H.-S. Park, and S.-W. Kang, J. Appl. Phys. **88**, 6327 (2000).

133. Y. Sakuma, S. Muto, K. Nakajima, and N. Yokoyama, Appl. Surf. Sci. **82/83**, 239 (1994).

134. J.-S. Park and S.-W. Kang, American Vacuum Society Topical Conference on Atomic Layer Deposition 2002, Seoul (2002).

135. J.-D. Kwon, J.-S. Park, and S.-W. Kang, American Vacuum Society Topical Conference on Atomic Layer Deposition 2002, Seoul (2002).

136. P. Mårtensson, M. Juppo, M. Ritala, M. Leskelä, J.-O. Carlsson, J. Vac. Sci. Technol. **B17**, 2122 (1999).

137. H.S. Lim, S.B. Kang, I.S. Jeon, G.H. Choi, Y.W. Park, S.I. Lee, and J.T. Moon, Jpn. J. Appl. Phys. Pt. 1. **40**, 2669 (2001).

138. S.-D. Ahn, H.-B. Lee, and S.-W. Kang, ,Jpn. J. Appl. Phys. Pt.1 **39**, 3349 (2000)

139. S.-D. Ahn, H.-B. Lee, and S.-W. Kang, Electrochem. Solid-State Lett. **3**, 186 (2000).

140. W. Besling, A. Satta, J. Schuhmacher, T. Abell, V. Sutcliffe, A.M. Hoyas, G. Beyer, D. Gravestejin, and K. Max, Proc. of the IEEE 2002 International Interconnect Technology Conference 288 (2002).

141. A. Satta, M. Baklanov, O. Richard, A. Vantomme, H. Bender, T. Conrad, K. Maex, W.M. Li, K.E. Elers, and S. Haukka, Microelectronic Engineering **60**, 59 (2002).

142. CRC Handbook of Chemistry of Physics, 71th Ed., edited by D. Lide, CRC, Boston, (1990).

143. K. Holloway, P.M. Fryer, C. Cabral Jr., J.M.E. Harper, P.J. Bailey, and K.H. Kelleher, J. Appl. Phys. **71**, 5433 (1992).

144. C.-K. Hu, S. Chang, M.B. Small, and J.E. Lewis, Proc. Third International VLSI Multilevel Interconnection Conference, IEEE Electron Devices Society 9, (1986)

145. L.G. Feinstein and R.D. Huttemann, Thin Solid Films **16**, 129 (1973).

146. L.A. Clevenger, A. Mutscheler, J.M.E. Harper, C. Cabral, Jr., and K. Balmak, J. Appl. Phys. **72**, 4918 (1992).

147. P.N. Baker, Thin Solid Films **14**, 3 (1972).

148. M. Trkula, in *Tantalum*, Proceed. Symp. 125th TMS Annual Meeting and Exhibition, Ed. E. Cen, A. Crowson, E. Lavernia, W. Ebihara, and P. Kumar, 309 (1996).

149. X. Chen, H.L. Frisch, A.E. Kaloyeros, and B. Arkles, J. Vac. Sci. Technol. **B16**, 2887 (1998).

150. A.E. Kaloyeros, X. Chen, S. Lane, H.L. Frisch, and B. Arkles, J. Mater. Res. **15**, 2800 (2000).

151. N. Terao, Jap. J. Appl. Phys. **10**, 248 (1971).

152. E. Eisenbraun, A. Upham, R. Dash, W. Zeng, J. Hoefnagels, S. Lane, D. Anjum, K. Dovidenko, A. Kaloyeros, B. Arkles, and J.J. Sullivan, J. Vac. Technol. **A18**, 2011 (2000).

153. H.-L. Park, K.-M Byun, and W.-J. Lee, Jpn. J. Appl. Phys. **41**, 6165 (2002).

154. S.-J. Park, K.-I. Na, W.-C. Jeong, S.-H. Kim, S.-E. Boo, N.-J. Bae, and J.-H. Lee, American Vacuum Society Topical Conference on Atomic Layer Deposition 2002, Seoul (2002).

155. H. Kim and S.M. Rossnagel, American Vacuum Society Topical Conference on Atomic Layer Deposition 2002, Seoul (2002).

156. B.H. Kim, K.I. Choi, H.S. Jung, S.B. Kang, G.H. Choi, J.H. Lee, U-I. Chung, and J.T. Moon, American Vacuum Society Topical Conference on Atomic Layer Deposition 2002, Seoul (2002).

157. H.S. Sim, Y.T. Kim, and H. Jeon, American Vacuum Society Topical Conference on Atomic Layer Deposition 2002, Seoul (2002).

158. W.-M. Li, K. Elerrs, J. Kostamo, S. Kaipio, H. Huotari, M. Soininen, P.J. Soininen, M. Tuominen, S. Kaukka, S. Smith, and W. Besling, Proc. of the IEEE 2002 International Interconnect Technology Conference 191 (2002)

159. J.A.T. Norman, J. Phys. IV France **11**, Pr3-497 (2001).

160. P. Mårtensson and J.-O. Carlsson, Che. Vap. Deposition **3**, 45 (1997).

161. P. Mårtensson, K. larsson, and J.-O. Carlsson, Appl. Surf. Sci. **136**, 137 (1998).

162. P. Mårtensson, K. larsson, and J.-O. Carlsson, Appl. Surf. Sci. **148**, 9 (1999).

163. P. Mårtensson and J.-O. Carlsson, Electochemical Soc. Proceedings, **97-25**, 1649 (1997).

164. J. Kostamo, V. Saanila1, M. Tuominen, S. Haukka, K.-E. Elers, M. Soininen, W.-M. Li, M. Leinikka, S. Kaipio, and H. Huotari, American Vacuum Society Topical Conference on Atomic Layer Deposition 2002, Seoul (2002).

165. J.S. Reid, E. Kolawa, C.M. Garland, M.-A. Nicolet, F. Cardone, D. Gupta, and R.P. Ruiz, J. Appl. Phys. **79**, 1109 (1996).

166. E. Eisenbraun, O. van der Straten, Y. Zhu, K. Dovidenko, and A. Kaloyeros, Proc. of the IEEE 2001 International Interconnect Technology Conference 207 (2001).

167. Y.-S. Suh, G.P. Heuss, and V. Misra, Appl. Phys. Lett. **80**, 1403 (2002).

168. D.-G. Park, T.-H. Cha, K-Y. Lim, H.-J. Cho, T.-K. Kim, S.-A. Jang, Y.-S. Suh, V. Misra, I.-S. Yeo, J.-S. Roh, J. W. Park, H.-K. Yoon, IEDM Tech. Digest 671, (2001).

169. S. Acquaviva, E.D'Anna, L. Elita, M. Fernandez, G. Legieri, A. Luches, M. Martino, P. Mengucci, and A. Zocco, Thin Solid Films **379**, 45 (2000).

170. J-S. Min, H.-S. Park, Y. Koh, and S.-W. Kang, Mat. Res. Soc. Symp. Proc. **564**, 207 (1999).

171. P.M. Smith and J.S. Cuter, Appl. Phys. Lett. **70**, 3116 (1997).

172. K.-E. Elers, M. Ritala, M. Leskelä, and E. Rauhala, Appl. Surf. Sci. **82/83**, 468 (1994).

173. S. Thompson, N. Anand, M. Armstrong, C. Auth, B. Arcot, M. Alavi, P. Bai, J. Bielefeld, R. Bigwood, J. Brandenburg, M. Buehler, S. Cea, V. Chikarmane, C. Choi, R. Frankovic, T. Ghani, G. Glass, W. Han, T. Hoffmann, M. Hussein, P.. Jacob, A. Jain, C. Jan, S. Joshi, C. Kenyon, J. Klaus, S. Klopcic, J. Luce, Z. Ma, B. Mcintyre, K. Mistry, A. Murthy, P. Nguyen, H. Pearson, T. Sandford, R. Schweinfurth, R. Shaheed, S. Sivakumar, M. Taylor, B. Tufts, C. Wallace, P. Wang, C. Weber, M. Bohr, 2002 Internation Electron Device meeting, Technical Digest. 61 (2002).

174. S. Saito and K. Kuramasu, Jpn. J. Appl. Phys. Pt. 1. **31**, 135 (1992).

175. J.G. Lee, S.K. Min, and S.H. Choh, Jpn. J. Appl. Phys. **33**, 7080 (1994).

176. H. Zhong, G. Heuss, Y.-S. Suh, V. Misra, and S.-N. Hong, J. Electronic Mat. **30**, 1493 (2001).

177. Y.J Lee and S.-W. Kang, Electrochem. Solid-State Lett. **5** C91 (2002).

178. D. Vogler and P. Doe, Solid State technology **46**, January, 35 (2003).

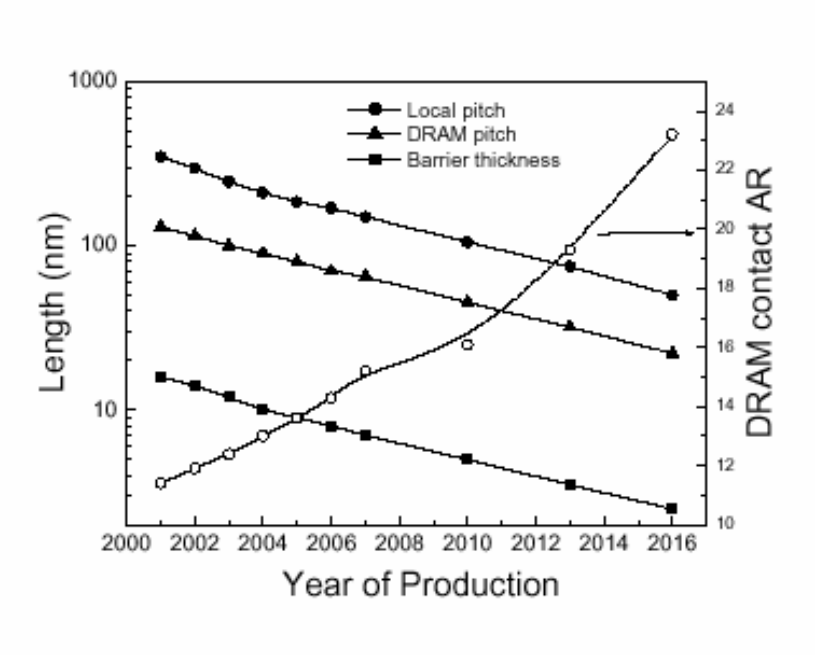


Fig. 1. The ITRS requirements (2001 edition) for interconnect structure as a function of year of production. The local pitch, DRAM pitch, and diffusion barrier thickness are represented by solid circle, solid triangle, and solid square and the aspect ratio for DRAM contact is represented by open circle.

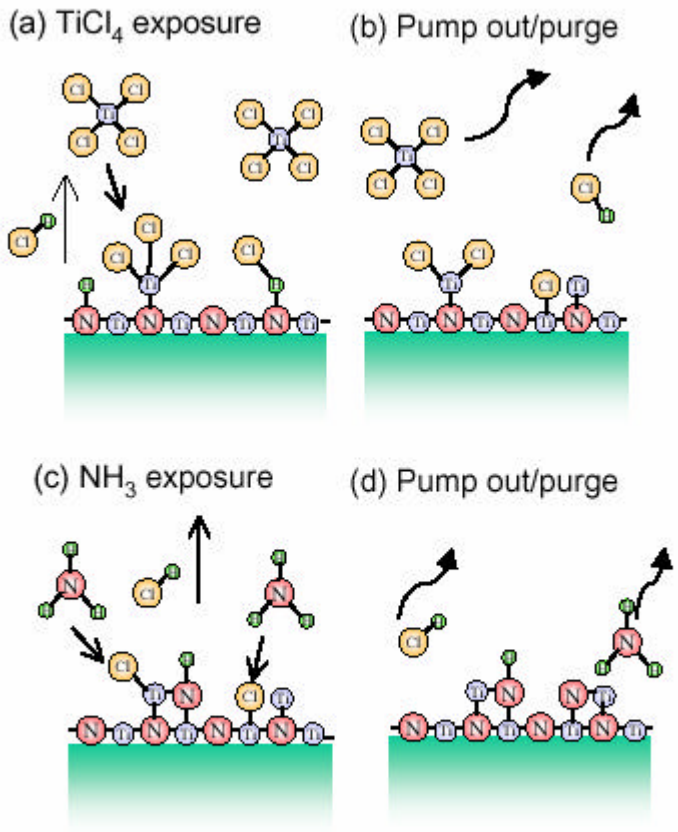


Fig. 2. The schematic representation of each process step for TiN ALD using $TiCl_4$ and NH_3 precursors. (a) $TiCl_4$ exposure, (b) pump out/purge, (c) NH_3 exposure, and (4) pump out/purge step.

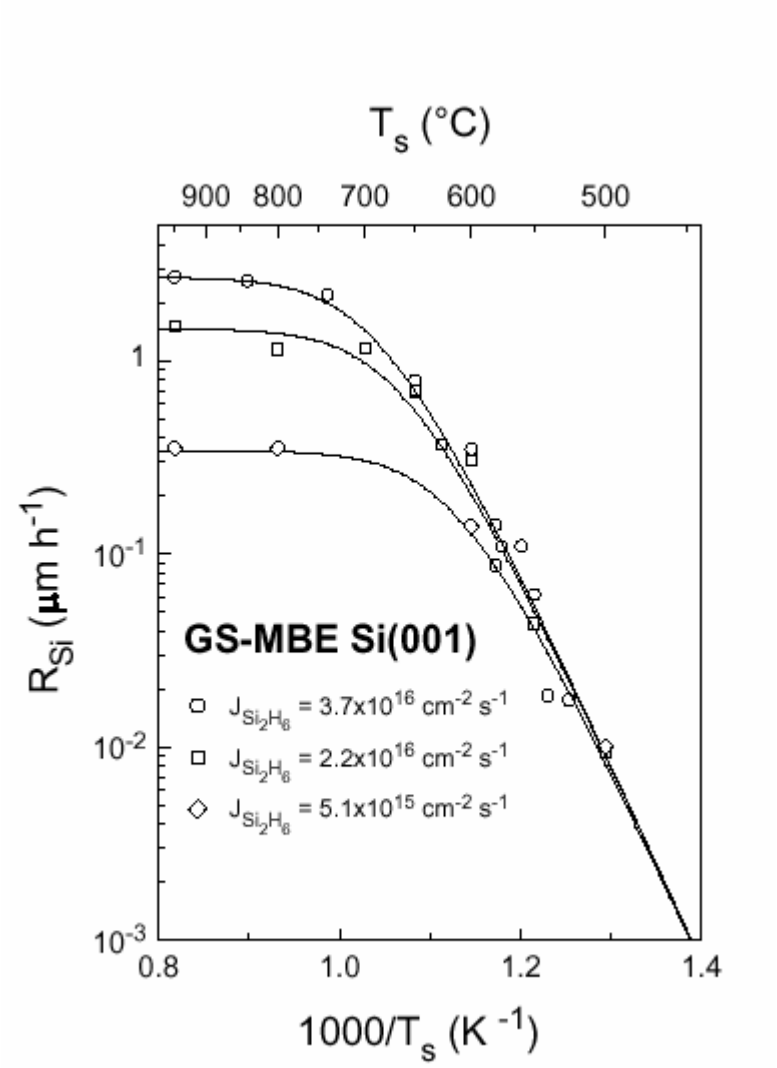


Fig. 3. The growth rate as a function of growth temperature for typical UHV-CVD type deposition of Si using Si_2H_6 precursor on Si(001) substrate.(Adapted from ref. 19)

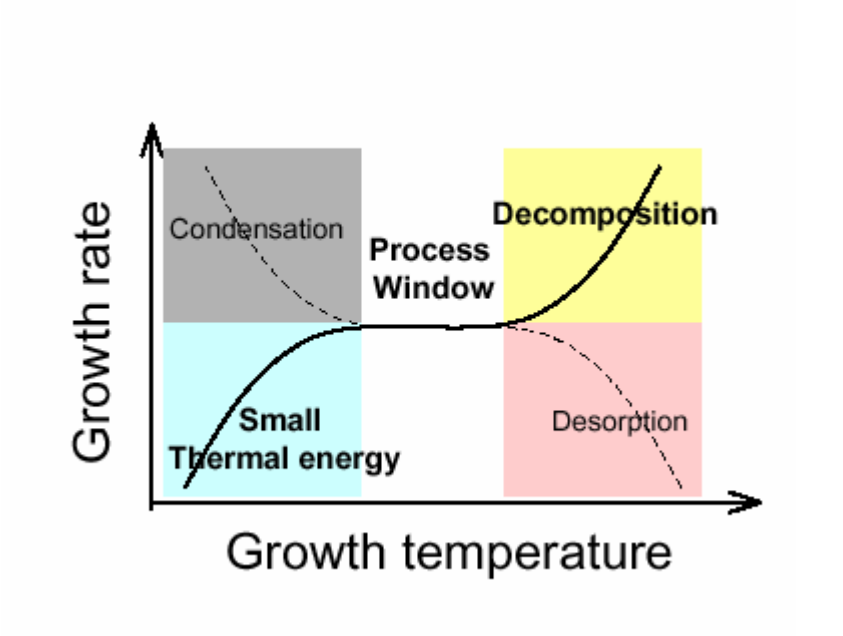


Fig. 4. The typical behavior of growth rate as a function of growth temperature for ALD process

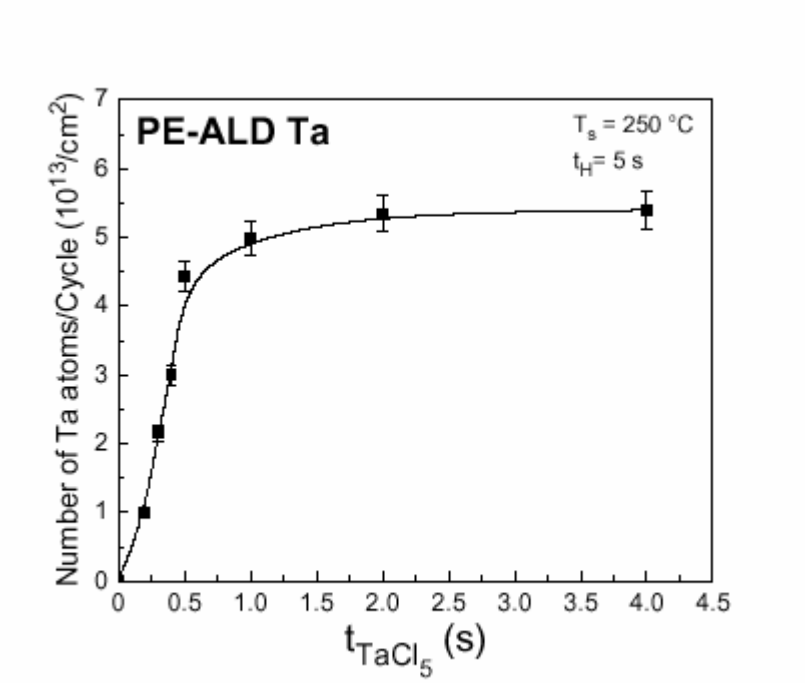


Fig. 5. The number of deposited Ta atoms per unit area as a function of $TaCl_5$ exposure time for PE-ALD Ta using $TaCl_5$ and atomic H as precursors, showing the saturation of $TaCl_5$ adsorption. The growth temperature was 250 °C and atomic hydrogen exposure time was 5 secs.

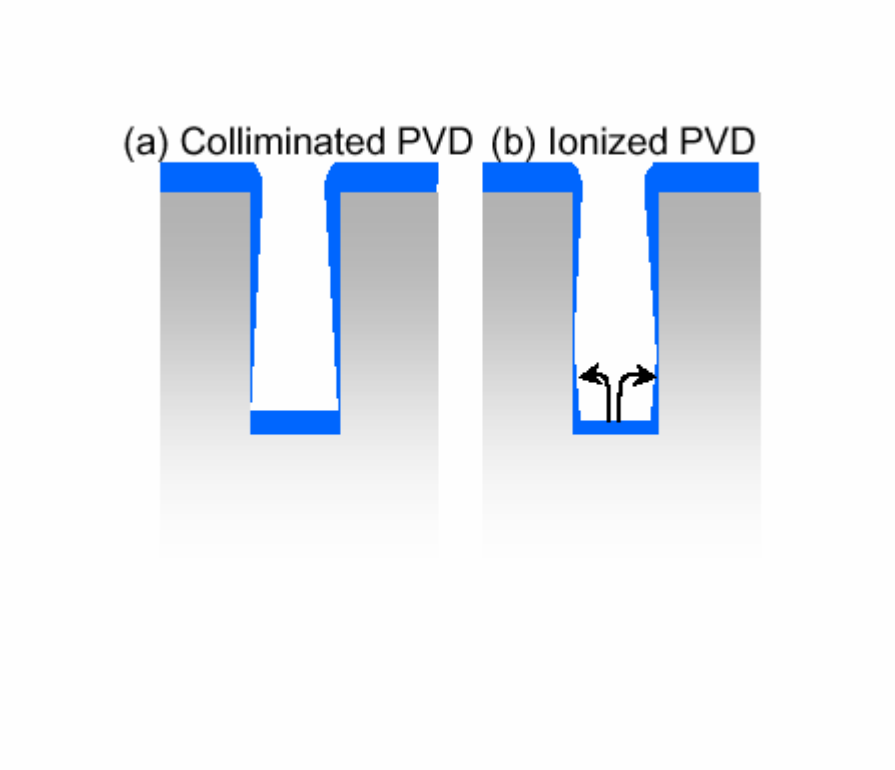


Fig. 6. The schematic drawing of deposited thin film profile of (a) collimated PVD and (b) ionized PVD on high aspect ratio deep trench/via structure.

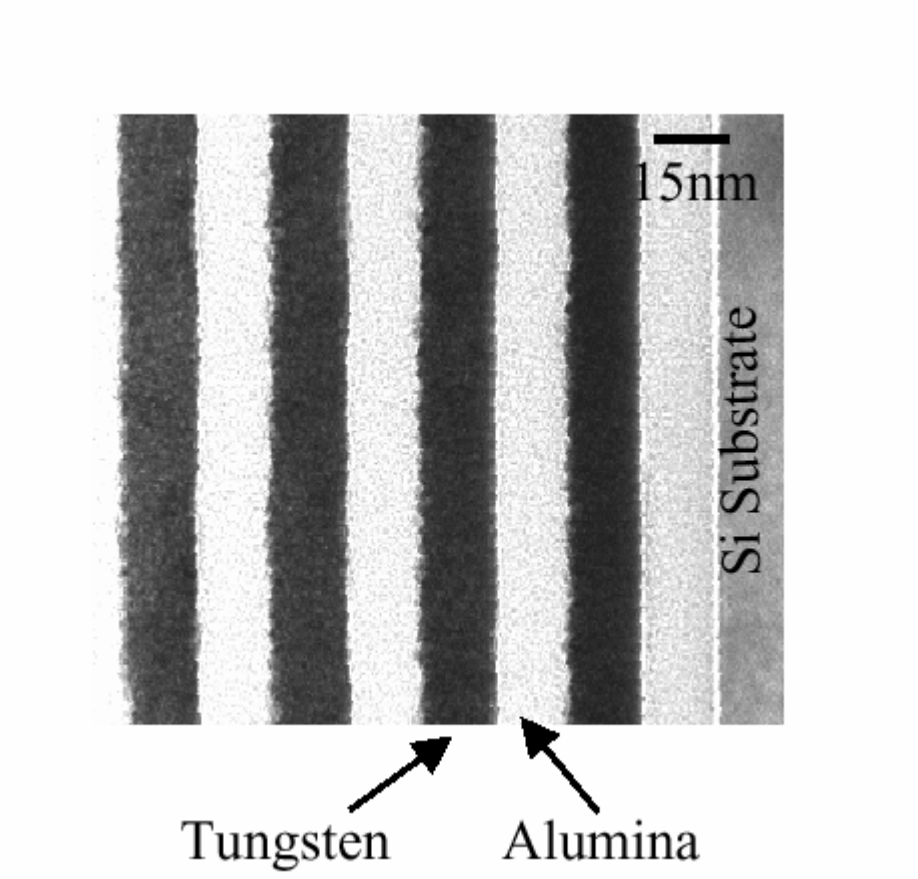


Fig. 7. TEM image of W-Al_2O_3 nanolaminate fabricated using ALD. The tungsten film was deposited using WF_6 and Si_2H_6.[31]

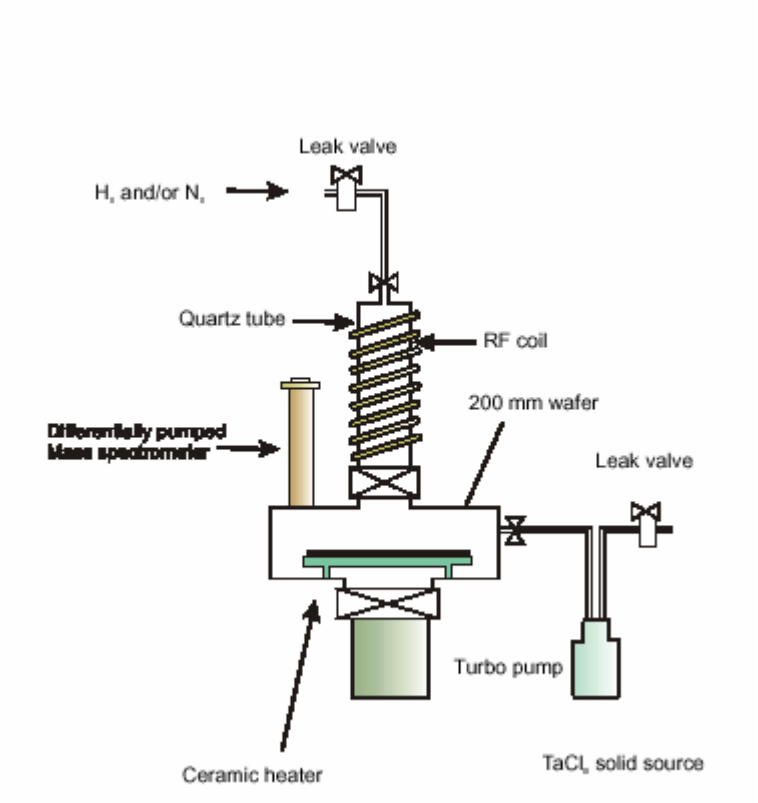


Fig. 8. A schematic drawing of rf-plasma based PE-ALD system used for PE-ALD of Ta and TaN thin films.

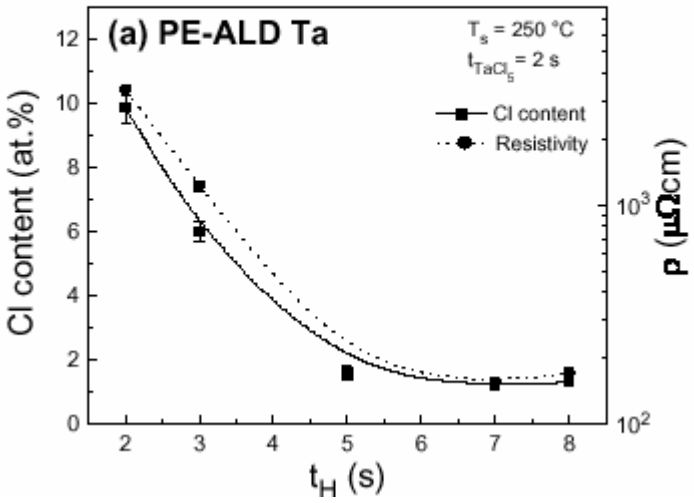


Fig. 9. The Cl content in PE-ALD Ta films grown with 2 secs of $TaCl_5$ exposure time as a function of (a) hydrogen plasma exposed time (t_H) at 250 °C and (b) growth temperature with t_H = 5 s. The Cl content and thickness were measured by RBS and sheet resistance by four point probe.

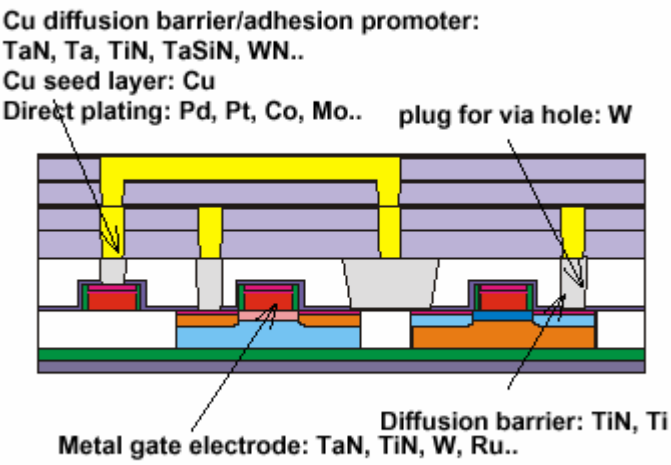


Fig. 10. The diagram showing the applications of ALD metals/nitrides and examples of materials studied for modern semiconductor devices.

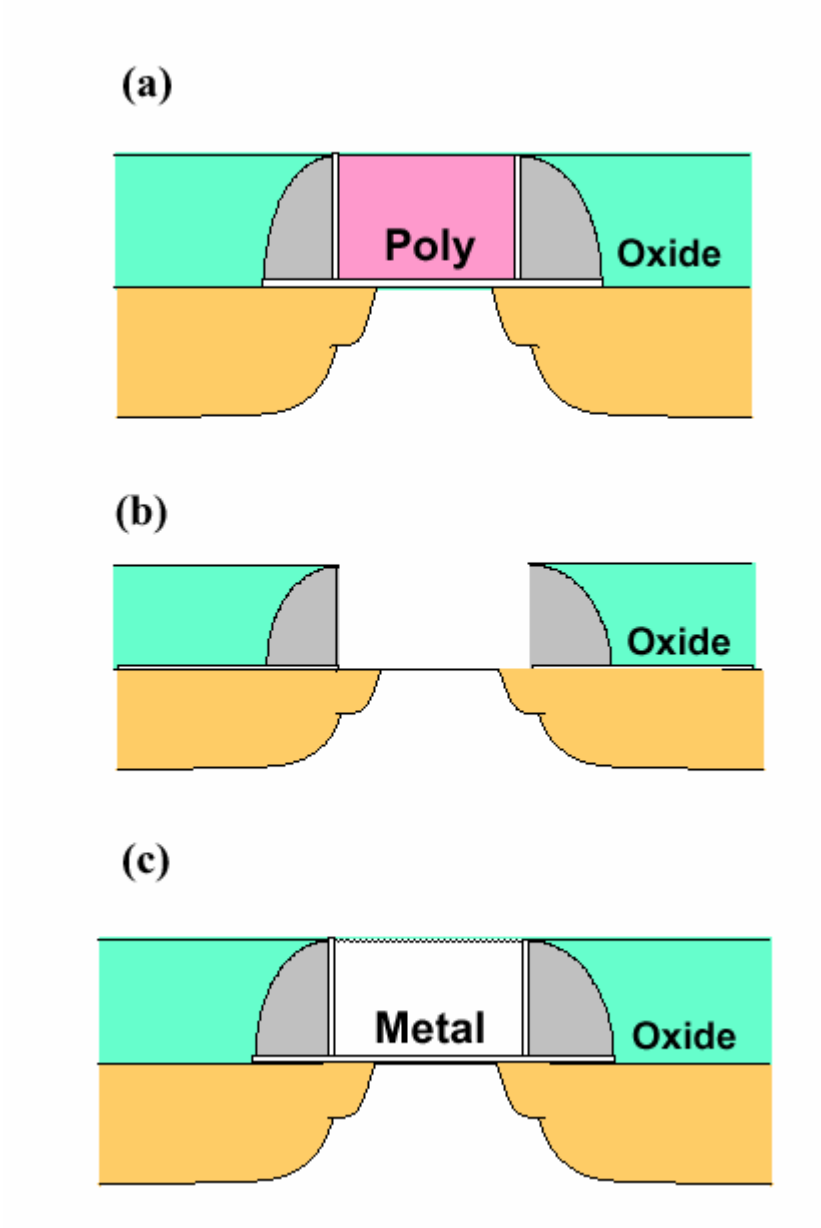


Fig. 11. The schematic diagram showing the typical process steps used for replacement gate integration scheme for CMOS device to implement metal gate electrode. The whole process consists of (a) conventional device fabrication and oxide CMP, (b) removal of sacrificial gate, and (c) gate oxidation, metal deposition and CMP.

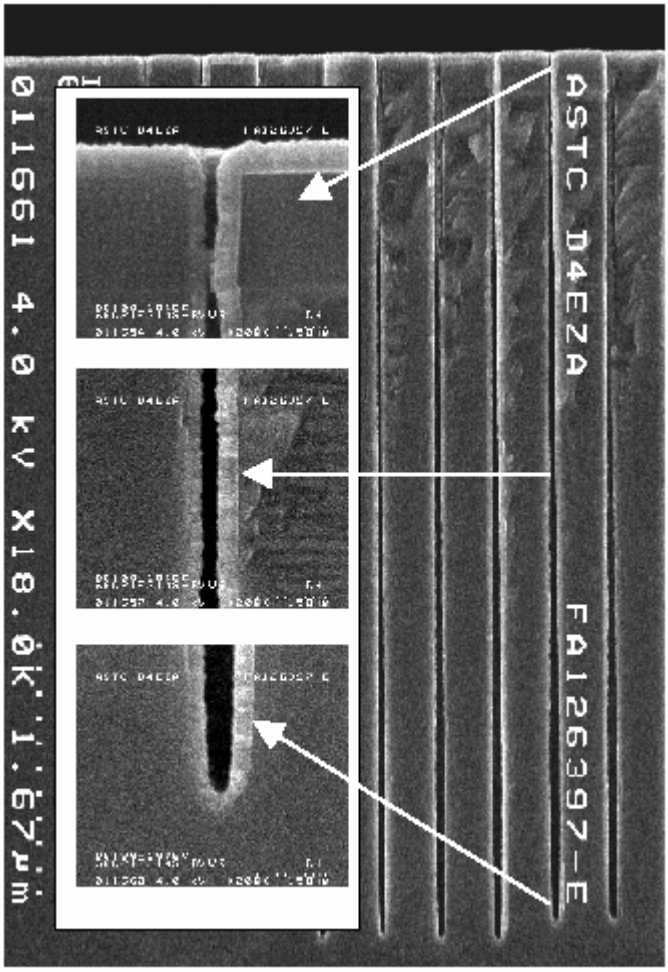


Fig. 12. ALD TiN film deposited inside the high aspect ratio trench capacitor showing excellent conformality of ALD process. The ALD has been performed by $TiCl_4$ and NH_3 as precursors.[96]

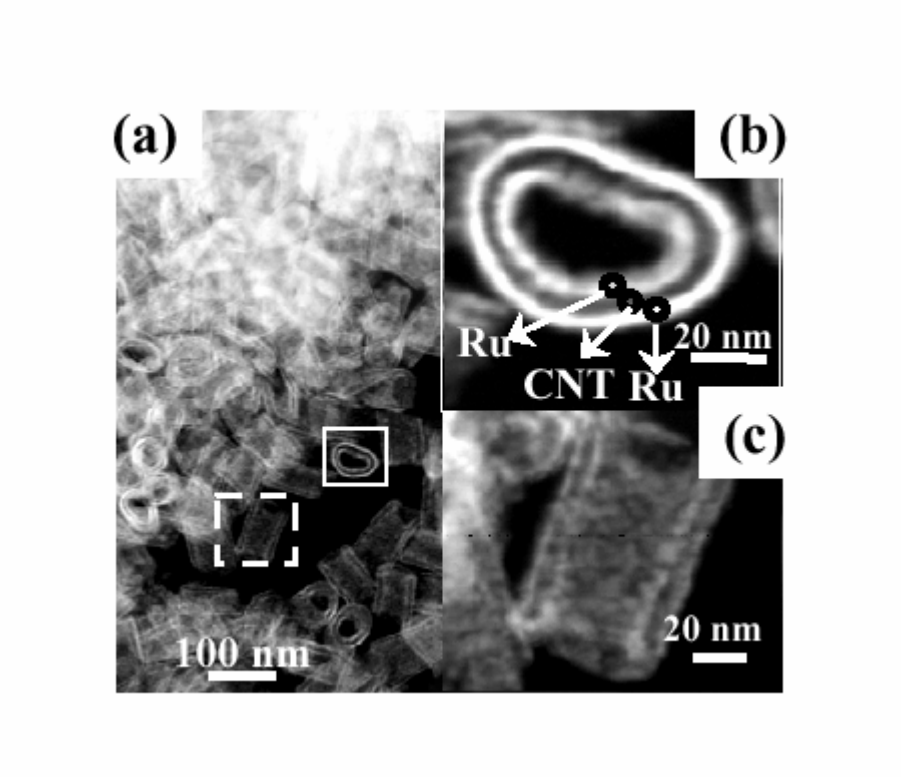


Fig. 13. (a) TEM image of Ru nanotube deposited by ALD using carbon nanotube template. $Ru(Od)_3$ and O_2 were used as precursors. (b) and (c) are magnified image of a single nanotube represented by solid square and dashed square, respectively, showing the top view and side view of nanotubes. (b) shows Ru films deposited outside and inside wall of carbon nanotube.[101]

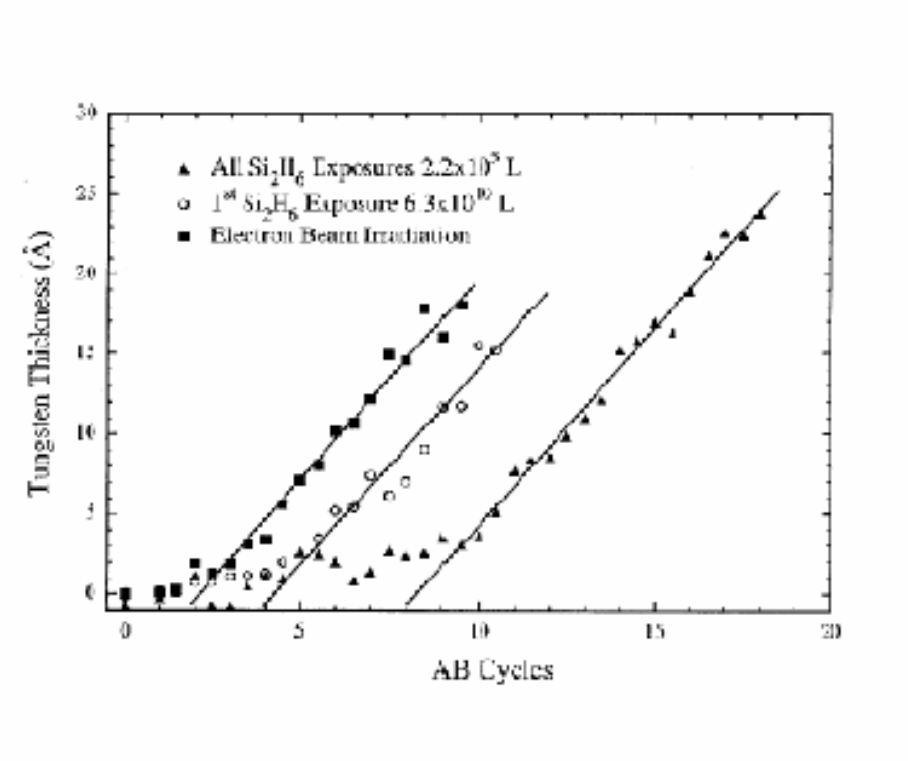


Fig. 14. The tungsten film thickness on SiO substrate by ALD from WF_6 and Si_2H_6 precursors as a function of number of cycles. The thickness was determined by AES O signal reduction and showing the nucleation period about up to 10 cycles. The nucleation period is shortened by higher exposure of Si_2H_6 or e-beam irradiation as represented by the open circles and solid squares.[102]

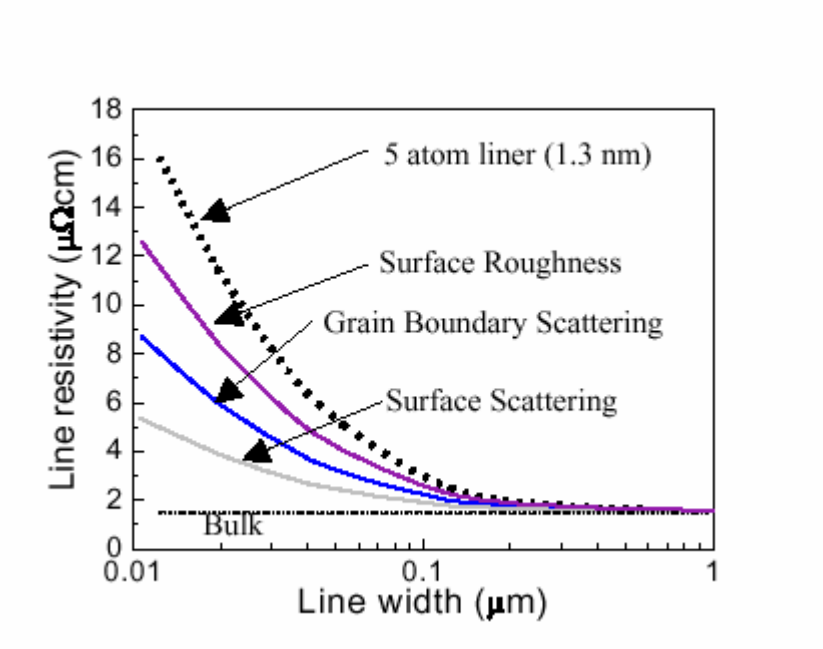


Fig. 15. Resistivity of Cu lines as a function of device feature size. The dotted line indicates the impact of adding a 5 atom thick liner on all 4 sides of a Cu line with the assumptions of grain size = linewidth and roughness = 5 nm.

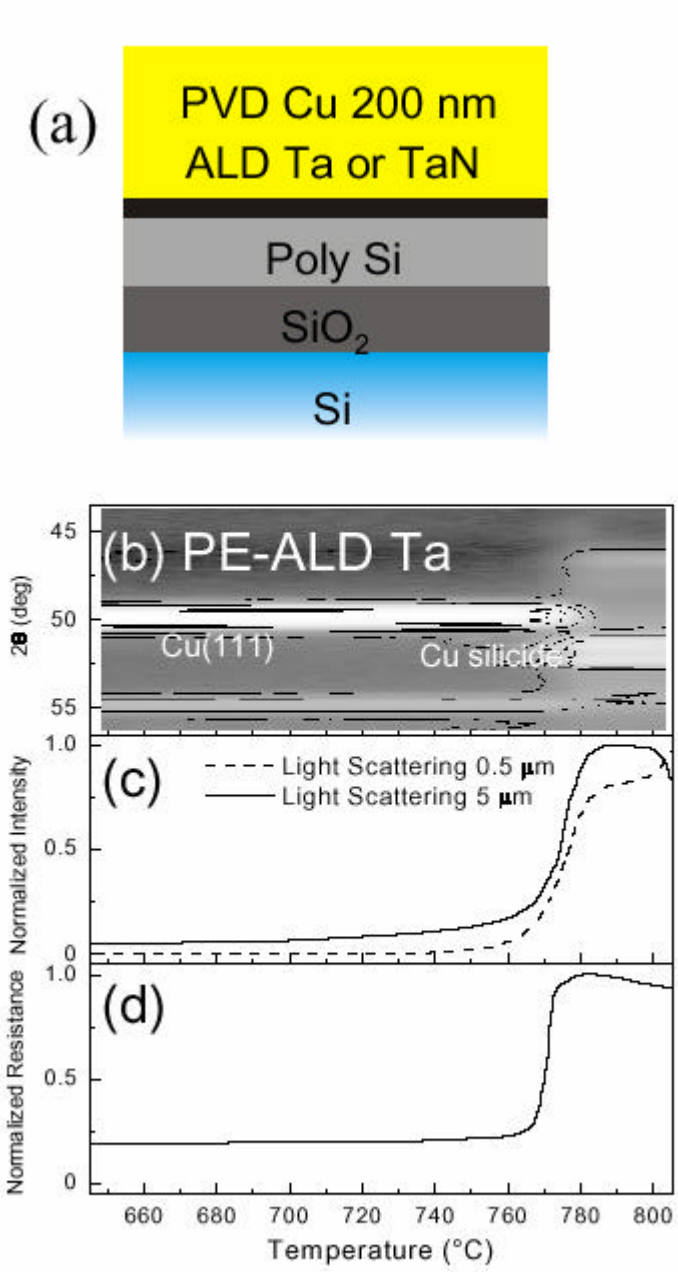


Fig. 16. (a) Diffusion barrier test structure and the results of three *in situ* analysis techniques, (b) X-ray synchrotron diffraction, (c) optical scattering, and (d) resistivity, for determining Cu diffusion barrier failure temperature for PE-ALD Ta deposited with $TaCl_5$ and atomic H with 7 nm thickness. [27]

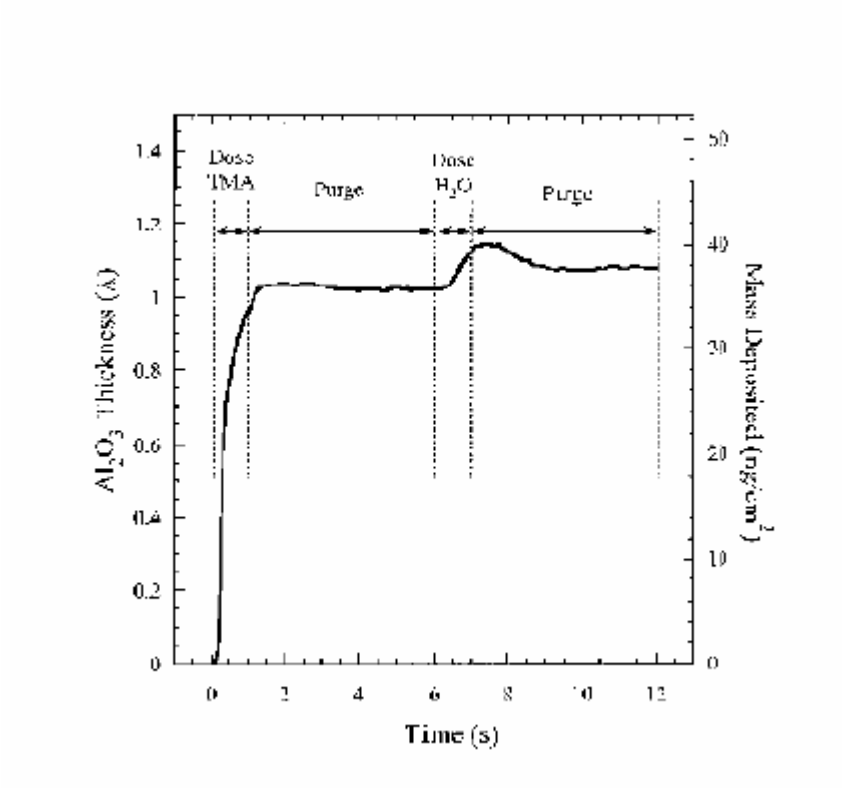


Fig. 17. Thickness measurement results by QCM for Al_2O_3 ALD using TMA and H_2O, showing the QMS signal as a function of each step of ALD. The majority increase in mass is observed for TMA adsorption step, with minor increase by H_2O exposure by formation of Al_2O_3.[112]

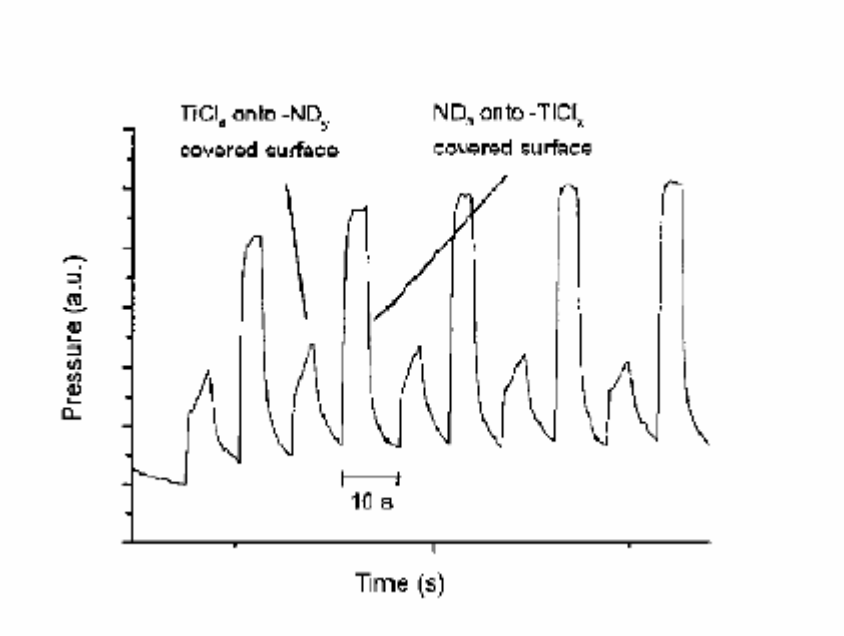


Fig. 18. The mass spectrometer signal of DCl by-product as a function of growth time during TiN ALD using $TiCl_4$ and ND_3. The exposure time for each precursor was 5 secs.[23]

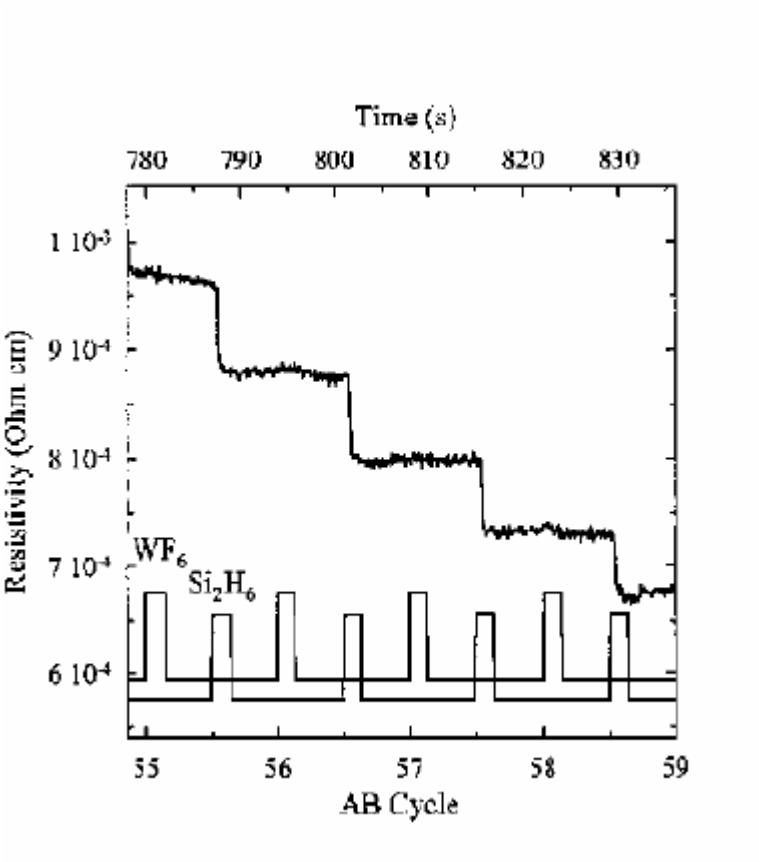


Fig. 19. The in situ resistivity measurements showing the reistivity change during W ALD from WF_6 and Si_2H_6 at 300 ºC. The exposure time for each precursors was 2s and purge time was 5 s.[123]

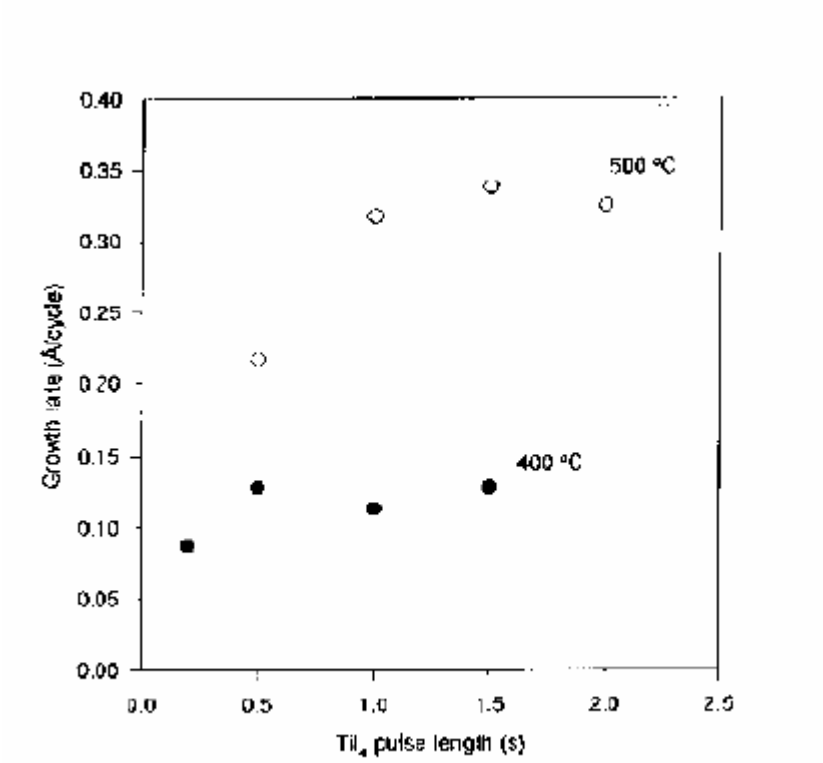


Fig. 20. The growth rate during TiI_4 ALD process from TiI_4 and NH_3 as a function of growth temperature showing that the higher growth rate was achievable at 500 ºC caused by the enhanced dissociation of TiI_4.[129]

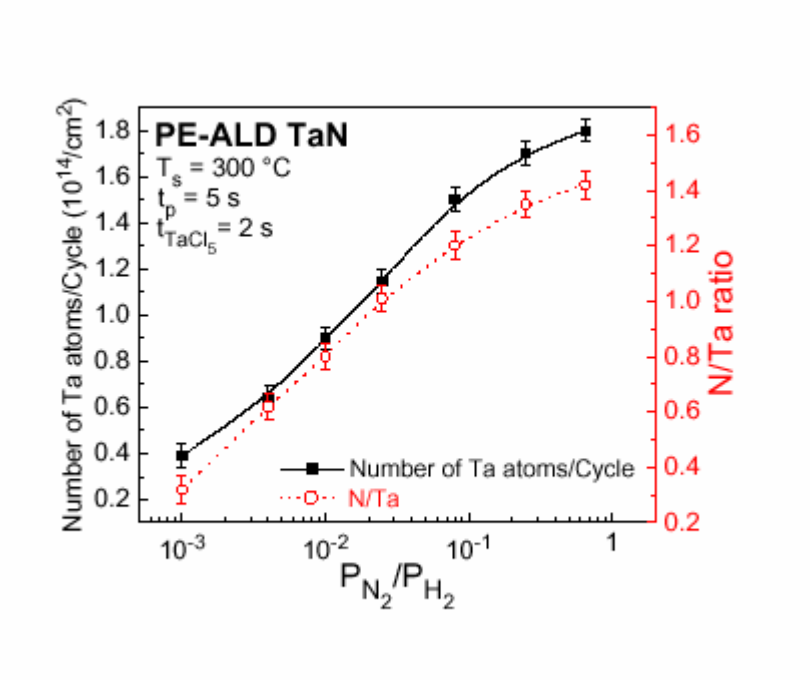


Fig. 21. The number of Ta atoms deposited per cycle and the N/Ta ratio in the film for PE-ALD TaN films grown from $TaCl_5$ and nitrogen/hydrogen plasma as a function of hydrogen/nitrogen partial pressure ratio during plasma exposure. The growth temperature was 300 ºC.[44]

Table 2.1. Comparison of thermal and plasma-enhanced ALD

	Thermal ALD	Plasma-Enhanced ALD
Benefits	- Simple chamber configuration - Simple reaction chemistry	- Low growth temperature - Higher density film - Lower impurity content
Reported materials	Metal: W, Cu, Ru, Pt, Ni Nitrides: TiN, TaN, Ta_3N_5, W_2N, MoN_x, NbN, $TiSi_xN_y$, $TiAl_xN_y$	Metal: Ti, Ta, Al Nitrides: TiN, TaN, $TiSi_xN_y$, $TaSi_xN_y$, W_2N

Table 2.2. Precursor combinations for metal/nitrides ALD

	Combination	Example
Metals	1. metal precursor + reducing agent	$TaCl_5 + H \rightarrow Ta$
	2. metal precursor + oxidant	$Ru(Cp)_2 + O_2 \rightarrow Ru$
	3. metal precursor + oxidant $\rightarrow$ reducing agent	$Ni(acac)_2 + H_2O \rightarrow NiO + H_2 \rightarrow Ni$
Nitrides	1. metal precursor + nitrogen source/reducing agent	$WF_6 + NH_3 \rightarrow W_2N$
	2. metal precursor + reducing agent	$TBTDET + H \rightarrow TaN$
	3. metal precursor + reducing agent + nitrogen source	$TaCl_5 + H + N_2^* \rightarrow TaN$
	4. metal precursor + nitrogen source/reducing agent + additional reducing agents	$TaCl_5 + NH_3 + Zn \rightarrow TaN$

Table 2.3. Reported metal precursors used for metals/nitrides ALD

		Precursors	Deposited materials
Inorganic (Halides)		$TaCl_5$, $TaBr_5$ $TiCl_4$,TiI_4 WF_6 $MoCl_5$ $NbCl_5$ CuCl	Ta, TaN, Ta_3N_5, $TaSi_xN_y$ Ti, TiN, $TiSi_xN_y$, $TiAl_xN_y$ W, W_2N, WC_xN_y Mo, MoN_x NbN Cu
Metal organic	Diketonato complexes	$Ni(acac)_2$ $Pt(acac)_2$ $Cu(hfac)_2$, $Cu(thd)_2$	Ni Pt Cu
	Cyclopentadienyl compounds	$Ru(Cp)_2$, $Ru(Od)_3$ $Me(Cp)Pt(Me)_3$ $Ni(Cp)_2$	Ru Pt Ni
	Alkyl compound	TMA	Al
	Alkylamides	TDMAT, TEMAT TBTDET, PEMAT	TiN, $TiSi_xN_y$, $TiAl_xN_y$ TaN

Table 3.1. Selected diffusion barrier materials

Metals		Ta, Ti, W, Cr, Co…
Metal alloys		TiW, NiNb…
Metal nitrides	Binary	TiN, TaN, Ta_2N, W_2N, HfN…
	Ternary	$TiSi_xN_y$, $TaSi_xN_y$, $TiAl_xN_y$, WSi_xN_y, WC_xN_y, WB_xN_y …

Table 3.2. Typical CMOS metal gate electrode materials

FET	Metals	Nitrides
n-FET	Ti, Ta, RuTa	TaN, $TaSi_xN_y$
p-FET	Pt, Mo, Ru	
Midgap	W	TiN

Table 4.1. *Ex-situ* analysis techniques employed for ALD of metal/nitirides properties.

Thickness (growth rate)	TEM, SEM, XRD, XRR, RBS
Composition/impurity content	RBS, XPS, AES, SIMS, EDX, NRD, FRES, MEIS
Microstructure	XRD, TEM
Conformality	TEM, SEM
Roughness	XRR, AFM, TEM
Electrical properties	Four point probe, C-V, I-V
Reliability test	Electromigration, stress migration

Table 4.2. Analysis techniques for diffusion barrier properties

Techniques	What to be measured	Representative reference
XRD	Formation of Cu silicide	58
Four point probe	Increase in resistance	27
Etch-pit test	Observation of developed etch pit on Si surface	107
Chemical analysis	Composition change, depth profiling	136
BTS	Flat voltage shift	17
C-V	Changes in electrical property	108
Optical scattering	Roughness change	27

Table 4.3. *In situ* analysis techniques for ALD of metal/nitirides.

Techniques	What to be measured	Studied materials and references
QCM	Mass change of the films	Ti[22]
Mass spectrometer	chemical species in the chamber	TiN, $TiAl_xN_y$ [23]
IR	Surface species	W, W_2N[25,117,120]
Ellipsometry	Film thickness	W, W_2N [25,117,120]
AES	Surface composition	W[102]
XPS	Surface composition	W[121]
Four point probe	Resistivity	W[123]

Table 5.1. Summary on reported results of TiN ALD

Metal Precursors	Other precursors	Growth temperature	Key properties	References
$TiCl_4$	NH_3	350 - 500 ºC	- Cl < 0.5 % (500 ºC) - ρ: 250 μΩcm (500 ºC)[16], 70 μΩcm (450 ºC)[15,18]	14-17
	DMHy	250 - 500 ºC	- C 13 %, Cl 2% (400 ºC)	67
	NH_3 +Zn	400 - 500 ºC	- ρ: 50 μΩcm (500 ºC)	16
	NH_3 + TMA	250 - 400 ºC	- Al 3 – 15 %, ρ: 140 μΩcm (400 ºC)	52
	allylNH_2 ^{t}BuNH_2 (+NH_3)	400 - 500 ºC	- Cl 1.4 %, ρ: 310 μΩcm (^{t}BuNH_2+NH_3, 400 ºC)	127
TiI_4	NH_3	400 - 500 ºC	- I <0.5, ρ: 70 μΩcm (500 ºC)	129
	^{t}BuNH_2 (+ NH_3)	400 - 500 ºC	- ρ: 150 μΩcm (^{t}BuNH_2 + NH_3, 400 ºC)	127
TDMAT	NH_3	180 ºC	- C, O > 10 %, ρ: 5000 μΩcm	55-57
TEMAT	NH_3	150 - 230 ºC	- C 4 - 10 %, ρ: 230 – 8000 μΩcm	54,58
TDMAT	H_2, H_2/N_2, N_2 plasma	150 – 350 ºC	- ρ: 300 - 500 μΩcm (for N_2 plasma) C, O < 3% (250 ºC with N_2 plasma)	70
$TiCl_4$	H_2/N_2/Ar Plasma	150 - 350 ºC	- Cl 0.5 %, ρ: 80 μΩcm(350 ºC)	134,135

Table 5.2. Summary on reported results of TaN ALD

Metal Precursors	Other precursors	Growth temperature	Phase	properties	References
$TaCl_5$	NH_3	200 - 450 ºC	Ta_3N_5	- Cl < 0.1%, ρ $5x10^5$ μΩcm (450 ºC)	14,26
	DMHy	300 - 400 ºC	Ta_3N_5	- Cl < 0.5 (400 ºC), ρ too high to be measured	67
	NH_3 +Zn	400 - 500 ºC	TaN	- Cl 4%, ρ: 900 μΩcm (400 ºC)	16
	NH_3 + TMA	250 - 400 ºC	Ta(Al)N(C)	- Cl 4%, C 26 %, Al 10 % (400 ºC)	68
	allylNH_2 ^{t}BuNH_2 (+NH_3)	350 - 500 ºC	TaN	- Cl 1.5%, C 11%, ρ: 1500 μΩcm (^{t}BuNH_2+NH_3, 500 ºC)	69
$TaBr_5$	NH_3	400 - 500 ºC	Ta_3N_5	- Br < 1%, ρ: 41000 μΩcm (500 ºC)	68
	NH_3 +Zn	400 - 500 ºC	TaN	- Br < 1%, ρ: 960 μΩcm (500 ºC)	68
	NH_3 + TMA	250 - 400 ºC	Ta(Al)N(C)	- Br 4%,Al 30%, ρ: 6600 μΩcm (400 ºC)	68
	^{t}BuNH_2 (+ NH_3)	400 - 500 ºC	TaN	- Cl 1.1%, C 7%, ρ: 2700 μΩcm (^{t}BuNH_2+NH_3, 500 ºC)	69
TBTDET	NH_3	260 ºC, 450 ºC	amorphous	- C 15 %, ρ > 10^6 μΩcm , density 3.6 g/cm^3[45,46]	45,46,152
	H_2 plasma	260 ºC	TaN	- C 15%, ρ: 500 μΩcm density 7.9 g/cm^3	45,46,
PEMAT	NH_3	250 ºC	amorphous	- C 7-8 %, ρ: 865200 μΩcm, density 8.4 g/cm^3	154
	N_2 plasma	250 ºC	TaN	- C 2-3 %, ρ: 30000 μΩcm, density 10.3 g/cm^3	154
$TaCl_5$	H_2/N_2 Plasma	100 - 400 ºC	TaN	- Cl < 0.5 %, ρ: 350 μΩcm, density 9.8 g/cm^3 (300 ºC)	27

Table 5.3. Summary on reported results of W and W nitride ALD

	Metal Precursors	Other precursors	Growth temperature	Key Properties	References
W	WF_6	Si_2H_6	150-430 ºC	- C, O < 4 %, ρ: 122μΩcm	25
		SiH_4*	300 – 400 ºC	- F < 0.2%, some Si	33
		B_2H_6	<300 ºC	- F < 0.01%	65
W_2N		NH_3	270-530 ºC	- W:N = 3:1, C, O < 5%, ρ: $4.5x10^6$ μΩcm	117
		NH_3	350 ºC	- W/N = 1.62, F <2.4, ρ: 4500 μΩcm	19
		NH_3 plasma	300-350 ºC	-	157
WC_xN_y		NH_3 +TEB	300 – 400 ºC	- C 35, N 15, F, O, B < 1, ρ: 350-400 μΩcm	158

* Pulsed layer nucleation

Table 5.4. Summary on reported results of Cu ALD

Metal Precursors	Other precursors	Growth temperature	Properties	References
CuCl	$Zn^{a)}$	440 – 500 ºC	- Zn: 3%, Cl<0.5% (500 ºC)	61
	H_2	360-410 ºC	- Cl 0.5% (410 ºC)	160
$Cu(hfac)_2 x H_2O$	Ethanol, Methanol, formalin	230-300 ºC	- C, O < 5% - ρ: 1.78 (formalin)– 5.33 (methanol) μΩcm	60
$Cu(acac)_2$	H_2	250 ºC	-	51
$Cu(thd)_2$	H_2	150-350 ºC	- C 19 % (350 ºC), ρ: 8 μΩcm	59
	$O_3^{b)}$	110-175 ºC	- C < 0.1%, ρ < 10 μΩcm,	164

a) ALD was not achieved.

b) by CuO reduction using ethanol

Table 5.5 Reported ALD process of ternary transition metal nitrides

Material	Precursors sequence	Growth temperature	Resistivity ($\mu\Omega$cm)	Refs.
$TiSi_xN_y$	$TDMAT+SiH_4+NH_3$	180 °C	30000	55,108,170
	$TiCl_4+SiH_4+ H_2/N_2$ plasma	350 ºC	500	134
$TaSi_xN_y$	$TaCl_5+SiH_4+ H_2/N_2$ plasma	300 ºC	1000	53
$TiAl_xN_y$	$TiCl_4$+ DMAH-EPP+ NH_3	350-400 °C	400	72
	$TDMAT+DMAH-EPP+NH_3$	200 ºC	1500 - 4700	73,74

Table 5.6. Reported ALD process for other metals/nitrides

Materials	Metal Precursors	Other precursors	Growth temperature	References
NbN	$NbCl_5$	NH_3	300 - 500 °C	14,67,126,172
		NH_3+Zn	500 °C	126,172
		DMHy	400 ºC	67
MoN_x	$MoCl_5$	NH_3	400 - 500 ºC	14,67
		NH_3+Zn	400 - 500 ºC	67
		DMHy	400 ºC	67
Mo	$MoCl_5$	Zn	400 – 500 ºC	64
Ni	$Ni(acac)_2$	H_2	250 ºC	51
		O_3 [a)]	250 ºC	51
	$Ni(Cp)_2$	H_2O,[b)]	150 ºC	66
Pt	$Pt(acac)_2$	H_2	250 ºC	50
	$MeCpPtMe_3$	O_2	275 – 450 ºC	49
Ru	$Ru(Cp)_2$	O_2	275 – 450 ºC	50
	$Ru(Od)_3$	O_2	200 ºC	101
Al	TMA	H_2 plasma	250 ºC	177

a) Reduction of ALD NiO by heating in 5%H_2/95%Ar at 230 ºC

b) Reduction of ALD NiO by hydrogen plasma